

A Model of the Electron

R. WAYTE

29 Audley Way, Ascot, Berkshire SL5 8EE, England, UK

e-mail: rwayte@googlemail.com

Submitted to Progress in Theoretical Physics, July 2010.

Abstract: A geometrical/mechanical model of the electron has been developed based on the measured fine structure constant, anomalous magnetic moment, and a solution of Einstein's equations of general relativity applied to electromagnetism. Properties such as charge, mass and spin have been explained from a classical viewpoint, and then α and μ calculated in agreement with experiment.

Keywords: theory of elementary particles and fields

1. Introduction

Physicists would be more comfortable with a real physical electron model, rather than the point-electron favoured by QED theory which employs a number of questionable techniques. Logically, if everything came from an original primeval particle consisting of a *single* material substance, then geometric extension and shape must be the distinguishing features between all observed bodies. So it would be improbable for the electron itself to have zero size and infinite density, while protons and atoms and everything else are extended.

For many years, there has been good reason to believe that electrons and nucleons have complex internal structures, although they may never be decomposed into stable, separate parts. For example, the measured spin and magnetic moment of an electron are real evidence for structure, even if in quantum theory they have been reduced to abstract parameters. Several investigators have proposed a spinning ring model of the electron with varying success and limitations; see a review with references at Wiki ¹⁾, including papers by Bergman & Wesley ²⁾, and Bostick ³⁾.

The toroidal ring electron model presented here is based on the universal solution of Einstein's equations of general relativity (Wayte)⁴⁾ applied to electromagnetism. Clearly, an electron with structure needs a more complicated description than a point-electron. However, the physical concepts required are very simple and everything is done with positive energy, forward running time and 3-dimensional empty space, from a geometrical/mechanical point of view. Overall, the electron has the appearance of a helically wound hollow torus, wherein the winding material is itself a thinner continuous helix, see Figure 1. Electron mass is the matter/energy which constitutes and runs through this structure at the velocity of light. This means that an electron behaves like a light-clock and undergoes relativistic time dilation and length contraction. The natural fine structure constant value will be defined by a formula which describes electron structure and its creation processes.

Characteristics of a good electron model will now be discussed briefly as a prelude to understanding the subsequent detailed model which satisfies experimental observation. It will be assumed that the classical laws of conservation of energy and momentum hold continuously with no failure periods, and the electron as a whole must behave in accordance with relativity theory. All physical constants and electron parameters have been taken from <http://physics.nist.gov/constants> and <http://pdg.lbl.gov>.

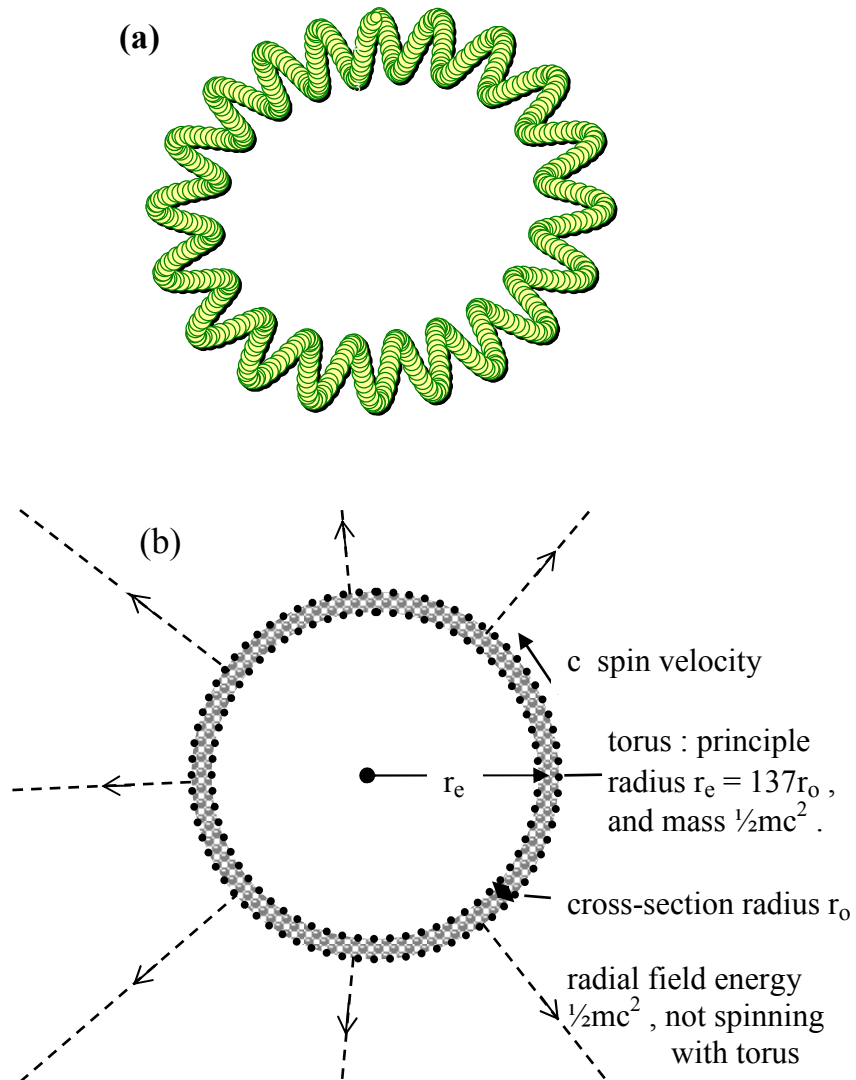


Fig 1 (a) General illustration of toroidal electron, with its helix-upon-helix structure. (Not to scale).
 (b) Schematic diagram of the overall electron model, with half the electron energy in a spinning torus and the other half in a radial electromagnetic field. (Not to scale)

1.1 Charge and the electromagnetic field. Charge is regarded as being due to the existence of a real electromagnetic field of energetic quanta emitted by a particle. These quanta are tied to their particles to conserve energy, but propagate out and back at the

velocity of light. When a field quantum from one particle interacts with a field of another particle it is either deflected away or attracted towards that particle, according to whether the two particles are of similar charge or opposite. This deflection causes momentum exchange and epitomises the force mechanism, (see Wayte 1983⁴), p.358, for the gravitational analogue).

The field quanta of opposite charges do not sink in each other's particles, as lines of force are often depicted. That would result in depletion of the far field strength and lead to disagreement with the standard dipole field calculation. Consequently, a neutral hydrogen atom must have superimposed positive and negative electromagnetic fields which neutralise in force but add in energy density.

1.2 Mass, potential energy, and kinetic energy. For opposite charges, the field is only inductive and causes motion but no energy exchange occurs, as was found in gravitation theory. Then for example, a positron and electron at rest kilometres apart may attract each other and fall together by converting their own rest mass energy to kinetic energy. Upon collision, two identical photons are emitted of total energy $2h\nu = m_{o(+)}c^2 + m_{o(-)}c^2$. During the fall, at separation r we have (in cgs units for simplicity):

$$2\left(\frac{e^2}{r}\right) = 2(m_o c^2 - m_r c^2) = 2\left\{\frac{m_r c^2}{\left(1 - v^2/c^2\right)^{1/2}} - m_r c^2\right\}, \quad (1.1)$$

[coordinate
[coordinate
[coordinate
PE lost]
rest mass lost]
KE gained]

where $m_r = m_o(1 - e^2/m_o c^2 r)$ is the coordinate rest mass. Evidently, potential energy is the same thing as rest mass energy, and may convert to kinetic energy of the same particle.

To make charges of the same sign approach each other, it is necessary to increase their kinetic energy by means of a separate external field. In a head-on collision, this KE converts to rest mass energy as the particles slow during flight to zero velocity. Then at the distance of closest approach (R) we have:

$$2 m_o c^2 + 2\left(\frac{e^2}{R}\right) = \frac{2 m_o c^2}{\left(1 - v_1^2/c^2\right)^{1/2}} = 2 m_1 c^2, \quad (1.2)$$

where the left side is total rest mass energy, and on the right side is the relativistic initial rest mass plus kinetic energy. Again, potential energy (e^2/R) represents rest mass energy. Equation (1.2) is very interesting because R may decrease as necessary when v_1 approaches c in particle accelerators. However, the electron radius also decreases as its kinetic energy increases, ($r_{01} = e^2/m_1c^2$). In addition, during a high energy collision, the effective electron charge increases to cause apparent running of the fine structure constant. This all makes the electron behave point-like, in spite of its finite structure.

Given that an electron and positron may be created as a pair from pure energy, and they are identical except for charge, then only their shape in the form of helicity can distinguish between them. This means that their field quanta have opposite helicity, left for electron and right for positron. For compatibility, their internal mechanisms probably have the same helicity as their fields. According to general relativity theory (Wayte pp.349-353)⁴⁾, field quanta have equal radial and tangential momenta, therefore unitary helicity; as follows.

If we let the electric potential energy function be $\gamma = (1 - e^2 / mc^2r)$, and define γ^2 as the metric tensor component, then Einstein's field equations for the electric field of a spherically-symmetric static electron may be written:

$$8\pi(E/c^4)T_1^1 = 8\pi(E/c^4)T_4^4 = \frac{1}{r^2} \frac{d}{dr} [r(1-\gamma^2)], \quad (1.3a)$$

$$-8\pi(E/c^4)T_2^2 = -8\pi(E/c^4)T_3^3 = \frac{\gamma}{r^2} \frac{d}{dr} \left(r^2 \frac{d\gamma}{dr} \right) + \left(\frac{d\gamma}{dr} \right)^2, \quad (1.3b)$$

where $\sqrt{E} = (e/m)$ is the electronic charge/mass ratio. Upon substituting γ , these simplify to:

$$T_1^1 = T_4^4 = \frac{e^2}{8\pi r^4}, \text{ and } T_2^2 = T_3^3 = -\frac{e^2}{8\pi r^4}. \quad (1.4)$$

The negative sign for T_2^2 means that the electric field quanta have tangential momentum which is orthogonal to the radial direction. The radial momentum density T_1^1 is equal to the energy density T_4^4 because the field quanta travel at the velocity of light c , with unitary helicity. Total energy of the field may be found by integration from the classical electron radius ($r_0 = e^2 / mc^2$) to infinity:

$$W_0 = \int_{r_0}^{\infty} 4\pi r^2 T_4^4 dr = \frac{e^2}{2r_0} = \frac{1}{2} mc^2 . \quad (1.5)$$

The other half of the electron's energy resides in its complex core mechanism, which is the source of the field. This agrees with the classical result for work done in assembling an electron from elemental charges, assuming that this work is retained to constitute field energy:

$$W = \int \int_q \frac{dq}{r} = \left(\frac{1}{2}\right) \left(\frac{e^2}{r_0}\right) = \left(\frac{1}{2}\right) mc^2 . \quad (1.6)$$

Such a result explains why renormalisation in quantum electrodynamics theory is effective using the classical electron radius r_0 . Of course, the need for renormalisation in a point-electron theory should be taken as evidence that the electron is not really a point, see Landau and Lifshitz p.90⁵⁾.

1.3 Spin angular momentum. We shall find that a ring electron body has the shape of a spinning torus, of principle radius ($r_e = 137 r_0$) and cross-section radius r_0 . The spin radius is r_e but only half the electron energy is in this torus and spinning at velocity c , because the other half is in the non-spinning radial electromagnetic field, see Fig.1. Angular momentum of the electron is therefore:

$$s = (m/2)cr_e = \hbar/2 , \quad (1.7)$$

as measured by experiments, and predicted by Dirac's theory⁶⁾ which does not cover structure. Evidently, electron *mass* is non-other than localised energy, of which half is in the torus, spinning at the velocity of light, and half is in a radial field of tied energetic quanta. Higgs bosons are unnecessary.

1.4 Magnetic moment. For the basic electron model of Eq.(1.7), the spin-loop would be expected to produce a magnetic moment of 1 Bohr Magneton,

$$\mu_B = \text{current} \times \text{area} = \left(\frac{e}{2\pi r_e / c}\right) (\pi r_e^2) = \frac{e\hbar}{2m} . \quad (1.8)$$

This value also comes from Dirac's electron theory, even though electron structure was not included therein.

When measured, the magnetic moment μ_e is found to be slightly greater than μ_B , the latest result being:

$$\mu_e / \mu_B = 1.00115965218111(74). \quad (1.9)$$

A great deal of effort has gone into explaining this ratio for the point electron in quantum electrodynamics theory. Our electron model in Section (3) produces an accurate expression which is relatively concise and easy to comprehend. For this summary, it will be approximated to:

$$\mu_e / \mu_B = 1.00115965218151 \approx \{1 + 1/[2\pi \times 137]\}, \quad (1.10)$$

which is explained as follows. In order to keep the charge particles in the spinning torus from flying apart due to mutual repulsion and centrifugal force, a guidewave quantum is predicted to exist around the torus as a continuous loop capable of confining them. This quantum interacts with any externally applied magnetic field in the same way as the charge, so the curly bracket on the right of Eq.(1.10) covers total effective circulating charge. The *self-interaction energy* of the electron around the spin-loop, as calculated by using the method of Eq.(1.6), will be attributed to the guidewave field. When normalised, this amounts to $[(e^2/2\pi r_e)/mc^2 = 1/(2\pi 137)]$.

1.5 Heisenberg's uncertainty principle and the Dirac electron. This extended electron has an average centre of mass, but its electromagnetic field quanta are emitted spontaneously from charge travelling around its periphery at the velocity of light. Consequently, interactions with other particles cannot be defined exactly, and it is possible to understand the meaning of Heisenberg's uncertainty principle. The two forms of the principle are usually stated:

$$\Delta p \Delta x \geq \hbar, \quad \text{and} \quad \Delta E \Delta t \geq \hbar. \quad (1.11)$$

From the previous sections, Δp could be $(m/2)c$, and Δx the spin-loop radius (r_e), then:

$$(m/2)cr_e = \hbar/2. \quad (1.12)$$

This is the same as the minimum uncertainty product for a free wave packet in one dimension, see Schiff, p60⁷⁾. The helical motion of material around the spin-loop prevents the location of the electron from being defined accurately during an interaction. Since the

material velocity is always c , this would explain why the Dirac electron analysis produces $\pm c$, (Dirac, p.262⁶).

1.6 Relationship to positrons, photons, neutrinos and neutrons. As stated previously, the positron and electron have equal status and are identical except for their helicity and are therefore mirror-images of each other. Both have positive mass /energy as can be confirmed by careful solution of Dirac's equations to exclude unphysical negative energies. A neutrino has spin ($1/2$) and is thought to be essentially like an electron with no field, hence charge. Its shape is expected to be toroidal, of radius ($r_v = \hbar c / 2E_v$), where E_v is its energy. A photon has unitary spin and is thought to be toroidal in shape with all its electric field energy wrapped around its periphery, except for an external guide quantum as suggested by interference phenomena. Major radius is ($r_{ph} = \lambda / 2\pi = \hbar c / E$), so the rotating photon field will modulate the fields of any surrounding charges at frequency (c / λ). A following paper will show how the empirical value for neutron magnetic moment may be accurately calculated from a model in which a proton is placed at the centre of a toroidal electron.

1.7 Wave/particle duality, de Broglie and Compton wavelengths. Charge particles spin around the electron toroidal periphery at the velocity of light in period ($\tau = 2\pi r_e / c$). So the periphery is equal to the Compton wavelength ($\lambda_c = h/mc$), and the electron's field will be modulated at frequency ($\nu_c = c / \lambda_c$). These are the characteristic wavelength and frequency of an electron. However, guidewave quanta are emitted in addition to standard field quanta and these also have the Compton wavelength, but a de Broglie wavelength ($\lambda_B = h/mv$) may be generated from this for a moving electron. A derivation will be presented elsewhere, showing how Doppler-shifted Compton frequencies may interfere to produce beating at the de Broglie frequency [$\nu_B = \nu_c(v/c)$]. The beat wavelength is that of de Broglie, ($\lambda_B = c/\nu_B$), and this real modulated guidewave is described by the quantum wavefunction ψ , in addition to any statistical interpretation of ψ .

1.8 Fine structure constant. Comprehension of the fine structure constant ($\alpha \approx 137.036^{-1}$) will be concomitant with the detailed magnetic moment analysis and will lead to a unique

structure for the inner mechanism of an electron. The ring electron grows by a radial factor 137 from a seed, and has the overall appearance of a continuous closed helix or toroidal coil, wherein the 137 turns themselves consist of a miniature helix. The turns of the toroidal helix grow like particles and for visualisation purposes, the word 'particle' is used loosely in describing the quantised behaviour of each turn of any continuous helix around a circumference. The major toroid is the spin-loop of radius r_e discussed above, and consists of 137 helical turns which are of radius r_0 . Each of these turns or core 'particles' then consists of 137 smaller pearl 'particles' around its periphery. These likewise have 37 smaller grain particles around their peripheries, such that each of these has 24 smaller mite particles around it; and finally, each of these has 50 elemental particles around it. Every 'particle' periphery consists of the turns of an open continuous helix and has an electromagnetic guidewave to confine the material of these helices in orbit. It is necessary to postulate all these consecutive stages because one stage leads to another in the magnetic moment analysis. For comparison, QED theory starts simplistically with a point electron, then introduces a very large number of perturbation correction terms in addition to questionable postulates. And it is common knowledge that mathematical singularities are expediently interpreted without physical rigour, for the sake of some quick but temporary solution. The apparent success of the QED point electron is partly due to the fact that a uniform sphere of charge behaves like a point source because of the inverse square law; and limiting integrals to the classical radius is physically correct in a real electron model.

In each stage here, the turn of a helix or 'particle' will be shown to grow from a smaller seed into its final size, starting with the spin-loop (r_e) so as to make room for the next smaller species (r_0), and so on downwards. Ultimately, only the very smallest species is the actual source of electromagnetic field quanta, so the electronic charge e consists of a single filament of (137 x 137 x 37 x 24 x 50) elemental charges along a string of matter, wound into 5 sizes of helix.

2. Fine structure constant ($\alpha = e^2 / \hbar c \approx 1/137.036$)

This dimensionless constant appears everywhere in atomic physics, determining the energies of photon emission and absorption. For example, the emission energies from hydrogen are given by:

$$h\nu = \alpha^2 \left(\frac{m}{2} \right) c^2 \left(\frac{1}{n_1^2} - \frac{1}{n_2^2} \right) . \quad (2.0.1)$$

This is the result of a particle energy equation being subjected to a de Broglie wave condition. The value of α is not specified at all, but it does relate the first Bohr orbit radius ($r_1 = \hbar^2/me^2$) to the electron Compton wavelength ($\lambda_c = h/mc$). We shall infer that α must be determined by the electron structure, in terms of a particle energy value ($mc^2 = e^2/r_0$) and a wave condition ($2\pi r_e = h/mc$). Thus given that α is dimensionless, it will be taken to represent the ratio of the classical electron radius r_0 to the spin radius r_e , independent of mass:

$$\alpha = \frac{r_0}{r_e} = \left(\frac{e^2 / mc^2}{\hbar / mc} \right) = \frac{e^2}{\hbar c} \approx \frac{1}{137.036} . \quad (2.0.2)$$

The reason for the particular value of α has never been explained, so an interpretation of the number itself will now be founded upon material structure of the electron, developed from first principles. This will entail a series of diminishing helical sub-structures, denoted as a circumference of a spin-loop 'O_e of radius r_e ; core-segment 'O₀ of radius r_0 ; pearl 'O₁ of radius r_1 ; grain 'O₂ of radius r_2 ; mite 'O₃ of radius r_3 ; and final element 'O₄ of radius r_4 .

2.1 Creation of an electron core-segment: spiralling first stage

Consider the formula

$$137/(1 + \ln 137) \approx \exp[\pi(1.00002)] . \quad (2.1.1)$$

Here, the remarkable simplicity of this, in which α , π and natural logarithm base e_n are closely bound, indicates an absolute condition for α .

It is interesting to know which components of Eq.(2.0.2) can vary to satisfy Eq.(2.1.1). Thus, if an electron is created in a spherically symmetric gravitational field with its spin axis aligned in the radial direction, then r_0 and r_e are not contracted by the field. Action h is an invariant quantity in the field but e^2 , c , and mc^2 are contracted by the same factor as time. Planck's constant is also fundamental in determining a photon's energy ($E = h\nu$), within or outside a field. It follows that in free space, the value of α may be set by e^2 and c only; and in a high energy collision it may appear to run with e^2 .

Creation of an electron is largely described by formula (2.1.1), according to our model, as follows. It will be interpreted as the result of some specific physical process, so we have to work back to find the original general description. Let \tilde{z} be the ratio of two lengths z and z_{os} , with maximum value ($\tilde{z}_{max} = z_0/z_{os} \approx 137$). The proposed general form of Eq.(2.1.1) may then be reduced, by taking logarithms, to:

$$[\ln \tilde{z} - \ln(1 + \ln \tilde{z})] \Big|_1^{137} \approx [\theta/2] \Big|_0^{2\pi}, \quad (2.1.2)$$

where θ is some angle. Differentiation of this equation yields:

$$\int_1^{137} \left\{ \frac{1}{\tilde{z}} - \frac{1}{\tilde{z}} \left(\frac{1}{1 + \ln \tilde{z}} \right) \right\} d\tilde{z} \approx \int_0^{2\pi} \left(\frac{1}{2} \right) d\theta. \quad (2.1.3)$$

These are finite integrals only, so that the integrands need not necessarily be equal for any instantaneous values of \tilde{z} or θ . Substitution of ($z/z_{os} = \tilde{z}$), and multiplying through by ($e^2/c = mcr_0$) produces a recognisable potential energy factor (e^2/z):

$$\int_{z_{os}}^{137z_{os}} \left\{ \frac{e^2}{z} \frac{dz}{c} - \frac{e^2}{z} \left(\frac{1}{1 + \ln z/z_{os}} \right) \frac{dz}{c} \right\} \approx \int_0^{2\pi} \left(\frac{m}{2} \right) cr_0 d\theta. \quad (2.1.4)$$

That is, e^2/z represents the potential energy of an electron in the field of another electron, distance z away. Now for ($dz = vdt$), this looks like a kind of action integral, where action = energy x time or angular momentum x angle, [Landau and Lifshitz (1983), Section 16].

Unfortunately, we can get no further with our model until z is defined more specifically. It is therefore postulated that Eq.(2.1.4) describes part of the creation of the electron core (r_0) mentioned in Eq.(1.5) above, such that the maximum value of z is the circumference of a free circular orbit, ($z_0 = 2\pi r_0$), and this core is the effective source of electronic charge e . Then z is to be the instantaneous length of a loop of electromagnetic material which swells smoothly from a seed with circumference ($z_{os} = 2\pi r_{os}$) to its final size ($z_0 = 137.036z_{os}$), see Fig. 2.1. The material of the expanding loop also has an instantaneous orbital velocity $v_z \leq c$, so that every part describes a locus which is a logarithmic spiral given by:

$$r = r_{os} \exp(\beta/2\pi). \quad (2.1.5)$$

Here, β is the spiral angle starting from $\beta = 0$ at time $t = 0$, and increases to 4.92 complete revolutions while satisfying a further relationship:

$$\beta r = ct \quad . \quad (2.1.6)$$

Now ($z = 2\pi r$) is the instantaneous circumference of the expanding loop, and the tangential velocity of its material is:

$$r \left(\frac{d\beta}{dt} \right) = \left(\frac{dz}{dt} \right) = v_z \quad . \quad (2.1.7)$$

which is the rate of increase in the loop circumference. In addition, from Eqs.(2.1.5) and (2.1.6) we can derive:

$$v_z = \frac{dz}{dt} = \frac{c}{(1 + \beta/2\pi)} = \frac{c}{(1 + \ln(z/z_{os}))} \quad . \quad (2.2.8)$$

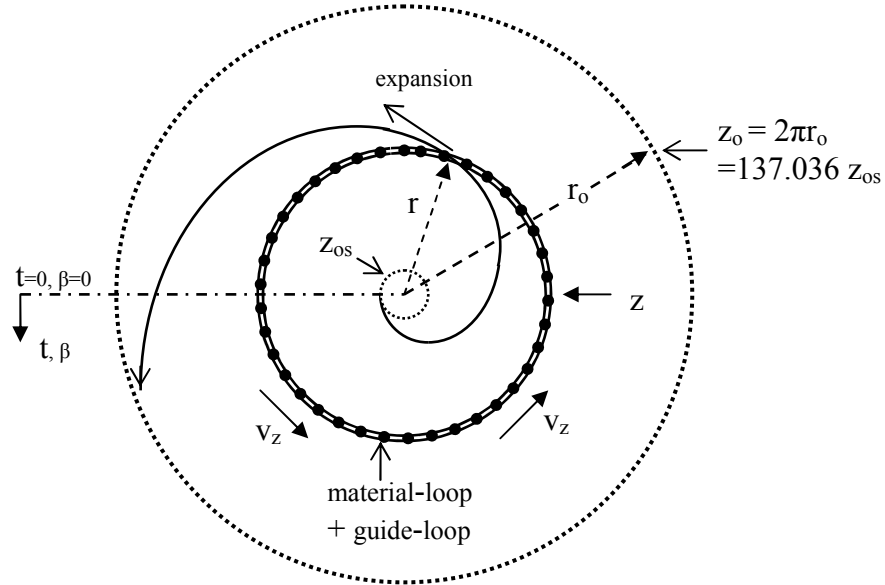


Fig 2.1 Schematic diagram of the core spiralling process in which the rotating material-loop expands exponentially from a seed radius r_{os} to its final radius r_o .

Before returning to Eq.(2.1.4) with this, we note one further aspect that ($\beta r = ct$) in Eq.(2.1.6) is also the distance around a circumference of radius r , which an electric field disturbance would travel at velocity c from $t = 0$ in order to meet up with the locus of the material at time t . This agrees with the proposal that the loop material continuously emits

and keeps in phase with a circulating electromagnetic field which guides and confines the material during its travel around the spiral.

The velocity v_z in Eq.(2.1.8) is of a useful form to substitute in Eq.(2.1.4) and get:

$$\int_{z_{os}}^{137z_{os}} \frac{e^2}{z} \frac{(1 - v_z/c)}{(1 - v_z^2/c^2)^{1/2}} \times \left[\frac{v_z}{c} \right] dt' \approx \int_0^{2\pi} \left(\frac{m}{2} \right) cr_0 d\theta \quad . \quad (2.1.9)$$

On the left, the integrand primary term is suggestive of a Doppler redshifted potential energy, due to expansion of the loop material. For this, the local time element [$dt' = dt(1 - v_z^2/c^2)^{1/2}$] has been introduced in place of coordinate time dt . An additional factor (v_z/c) is necessary because the electromagnetic energy is travelling here at velocity v_z rather than c , so the required local-time element is $(v_z dt'/c = dz'/c)$ rather than dt' . Thus the complete integrand has ultimately become an element of local action. And, given that action is Lorentz invariant, the whole integral is also *coordinate* action of the material potential energy throughout its spiralling stage of creation. On the right is a standard quantity of coordinate action for the final core kinetic energy over one internal revolution, of orbiting mass energy $(m/2)$ with velocity c at radius r_0 .

However, although at first sight Eq.(2.1.9) is a good description of the spiralling process, it is not entirely satisfactory from a physical viewpoint because at the spiral centre, the term (e^2/z_{os}) is greater than the total electron energy mc^2 . This problem does not arise if the core material actually consists of 137 core-segment 'particles', each of effective charge $(e/137)$. (They are actually the 137 turns of the toroidal helix described in Section 1.8). These core-segments, each of mass $m/137$, radius r_0 and period $(2\pi r_0/c)$, are to be spaced equally around the *spin-loop* such that the net electronic charge measured external to the complete system remains e . Then Eq.(2.1.9) can be made physically meaningful, and the correct action integral for the spiralling stage of creation of an *individual core-segment* becomes:

$$\int_{'O_{0s}}^{'O_0} \frac{(e/137)^2}{z} \left(1 - \frac{v_z}{c} \right) \left[\frac{v_z}{c} \right] dt \approx \int_0^{2\pi} \left(\frac{m}{2 \times 137^2} \right) cr_0 d\theta \quad , \quad (2.1.10)$$

where $'O_0$ and $'O_{0s}$ have now replaced z_0 and z_{os} as the specific nomenclatures for core-segment creation. To explain this new $(e/137)^2$ charge expression precisely, the material loop in the spiralling core-segment should consist of 137 pearl-seeds, which will later grow

into pearls. Then, every pearl-seed of charge $e/(137)^2$ interacts with the whole core-segment charge ($e/137$), to produce this given action in total for the core-segment's 137 pearl-seeds.

It is interesting to see how the pearl-seeds travelling at velocity v_z are controlled by their circulating electromagnetic field throughout the spiralling process. From Eq.(2.1.8) we derive:

$$\frac{(\beta + 2\pi)r}{\lambda_{osB}} = \frac{2\pi r}{\lambda_{osC}}, \quad (2.1.11)$$

where ($h_{os} = h / 137^2$) is to signify a primitive Planck's constant, so that ($\lambda_{osB} = h_{os} / mv_z$) is a primitive de Broglie wavelength, and ($\lambda_{osC} = h_{os} / mc$) is a primitive Compton wavelength. This expression means that the instantaneous position of each pearl-seed, with its emission of the circulating electromagnetic field, obeys a controlling wave equation throughout the expansion.

It is not obvious why in Eq.(2.1.10), the two independent finite action integrals should be equal, but we shall find that quantisation of action is always related to the number of quantum wavelengths within a given orbit: for example:

$$(m/2)cr_o 2\pi = (2\pi r_o / \lambda_{osC})(h_{os} / 2). \quad (2.1.12)$$

The core-segment material travels ($\ln 137.036 = 4.92$) times around the origin to reach its final radius r_o . The time t_m taken to do this is derivable from Eqs.(2.1.5) and (2.1.6) as:

$$t_m = t_{os}(137.036)\ln(137.036) = 674.25t_{os}, \quad (2.1.13)$$

where ($t_{os} = \alpha 2\pi r_o / c$) is the original core-segment-seed period. A feature of the creation action Eq.(2.1.10) is that it is independent of this creation period t_m , for this particular spiral shape.

Angular momentum of the material increases during the spiralling process by a factor of around 23. This can only mean that spin is introduced as necessary by interaction with the other creation participants within the electron, or externally such as a positron.

2.2 Creation of an electron core-segment: accelerating second stage

Thus far we have been describing how the electron core-segment material, containing 137 pearl-seeds, expands from its original orbit of radius r_{os} to an orbit of radius r_o by way of a spiralling process. But while achieving this radius, the material orbital

velocity has fallen from c to $c/(1+\ln 137)$ according to Eq.(2.1.8); so it is necessary to continue the creation beyond the spiralling stage by accelerating the material back to velocity c while at constant radius r_o .

The analysis of this accelerating second stage is more easily understood by first describing the design of the finished core-segment with its fully developed pearls, as follows. Consider the formula:

$$\alpha^{-1} \approx 137 \approx \exp(\pi^2/2), \quad (2.2.1)$$

or more accurately in logarithmic form:

$$\ln(137.036) \approx (\pi^2/2)(1-0.003). \quad (2.2.2)$$

Again, the simplicity of this formula indicates an absolute foundation for α and it will be taken as describing an end result; so once more the problem is to work back to the original description of some simple physical model. Let \tilde{y} be the ratio of two lengths y and y_o with maximum value ($\tilde{y}_{\max} \approx 137$), then the proposed general form of Eq.(2.2.2), which will lead to the final equilibrium state of the core-segment is:

$$\left(\frac{2}{\pi}\right) [\ln \tilde{y}]_1^{137} \approx \left[\frac{\theta}{2}\right]_0^{2\pi}. \quad (2.2.3)$$

Here, θ is the azimuthal position angle within the core-segment, of any given pearl, see Fig. 2.2. Length y_h is to be the orthogonal helical path length for a spinning pearl, starting from unit value ($y_o = 2\pi r_1' = 'O_1$), where the pearl radius is ($r_1' = (\pi/2)\alpha r_o$). Differentiation of Eq.(2.2.3) and multiplying through by ($e^2/c = mcr_o$) produces:

$$\int_{y_o}^{137y_o} \frac{e^2}{y_h} \frac{dy}{c(\pi/2)} \approx \int_0^{2\pi} \left(\frac{m}{2}\right) cr_o d\theta. \quad (2.2.4)$$

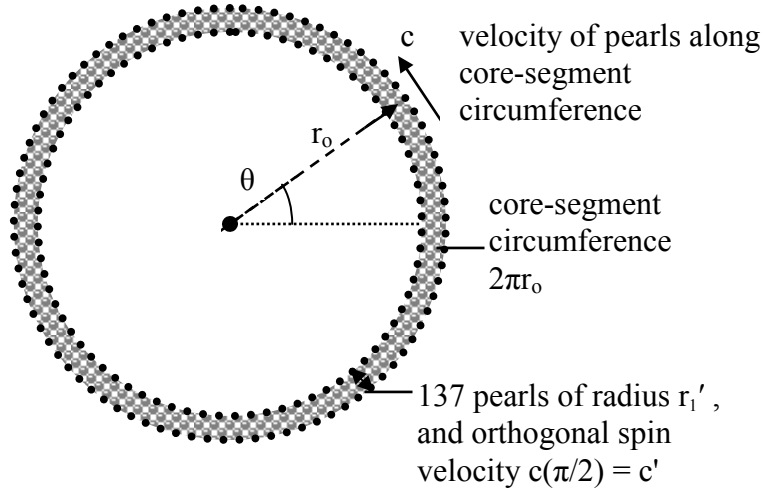


Fig 2.2 Schematic diagram of the core-segment in final equilibrium at radius r_0 , in which the 137 pearls of radius r_1' spin around the circumference describing a helix as they travel along.

The left hand side is a kind of action-integral for scalar potential energy. To account for factor $(\pi/2)$ it is proposed that the pearls spin around the core-segment circumference in a helix, with velocity $(\pi/2)c$ orthogonal to the θ plane as they travel along the circumference at velocity c . There are 137.036 turns over the circumference $2\pi r_0$, in period t_0 , so $[dy_h = (\pi/2)c dt]$. Upon introducing the pearl number 137 and the correct pearl charge $(e/137^2)$ as for Eq.(2.1.10), equation (2.2.4) reduces to an action-integral which describes a core-segment's complete pearly helix in its final equilibrium state:

$$\int_{y_0}^{137y_0} \frac{(e/137)^2}{y_h} dt \approx \int_0^{2\pi} \left(\frac{m}{2 \times 137^2} \right) c r_0 d\theta = \left\{ \left(\frac{m}{2 \times 137^2} \right) c^2 t_0 \right\} . \quad (2.2.5)$$

Here, the left hand side is the scalar potential action involved in taking the 137 charged pearls along their helical path around the core-segment periphery $2\pi r_0$. The right hand side is the equivalent kinetic action over the core-segment period ($t_0 = 2\pi r_0 / c$), which is numerically the same as in Eq.(2.1.10), for the spiralling action. This quantity of action must be fundamental because it will occur frequently in the following analysis.

Although the pearl's rotational velocity $(\pi/2)c$ may appear to contradict the theory of relativity it should be remembered that only the electron as a whole must obey that theory. In fact an electron with any structure whatsoever is bound to contain parts which move at velocities greater than c .

Given this final state description of a core-segment, it is now possible to advance the second stage creation mechanism which follows on from where spiralling equation (2.1.10) stops and leads eventually to Eq.(2.2.5). It will be shown later that the pearl-seeds grow into pearls proper during this acceleration period, but this does not influence the acceleration itself. So during this stage, it is proposed that the pearl(-seeds) are accelerated by an electromagnetic loop as was emitted throughout the spiralling process, but here the loop has constant length $2\pi r_0$, see Fig.2.3. The velocity is to increase from $[u_0 = c / (1 + \ln 137)]$ to velocity c , in a simple manner over a time t_0 say. Various ways of doing this may be proposed, but one way produces a good overall 'action' result. Namely, let the acceleration A be constant so that the general velocity of the pearl(-seeds) would increase linearly with time from zero as:

$$u = At \quad , \quad (2.2.6a)$$

and the corresponding distance travelled would be:

$$x = At^2 / 2 \quad . \quad (2.2.6b)$$

If the acceleration time is actually t_0 from u_0 to c , then the acceleration must be:

$$A = \frac{c}{t_0} \left[\frac{\ln 137}{1 + \ln 137} \right] \quad . \quad (2.2.7)$$

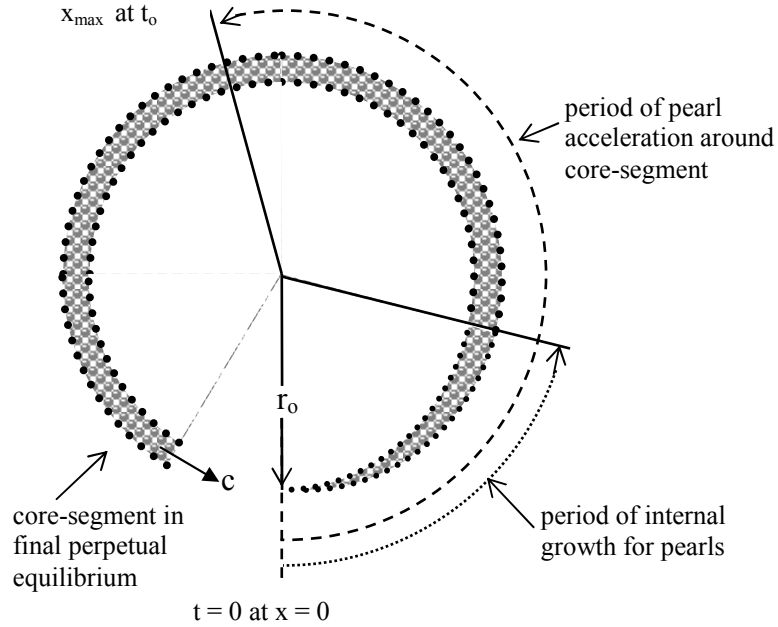


Fig 2.3 Schematic diagram of the core-segment acceleration process in which the rotating material at radius r_0 accelerates from velocity $c/(1+\ln 137)$ to c in time t_0 over a distance $2\pi r_0(0.58)$.

From this we may calculate the scalar potential action of the 137 pearl(-seeds) during the acceleration period. Given ($dt = dx/u$), then the action integral is:

$$\int_x \frac{(e/137)^2}{x} dt = \frac{e^2}{137^2 c} (2 \times \ln 137) \quad . \quad (2.2.8a)$$

It is interesting that the acceleration period was set arbitrarily as t_0 , but this integral happens to be independent of time. This result is also independent of the pearl's state of growth, and we shall see in Section (2.5) how the pearls grow completely during the earliest part of this core-segment acceleration stage, as drawn in Fig.2.3.

This action integral happens to be double the scalar potential action of the circulating electromagnetic field which propagates at velocity c around the core-segment circumference, to confine the 137 pearls in equilibrium:

$$\frac{e^2}{137^2 c} (2 \times \ln 137) = 2 \times \int_{2\pi r_0/137}^{2\pi r_0} \frac{(e/137)^2}{\zeta} \frac{d\zeta}{c} . \quad (2.2.8b)$$

The pearls are thus the source of "charge" in that they sustain the electron's electromagnetic field while travelling around the core-segments. This motion of pearls around each of the 137 core-segments travelling around the spin-loop will produce a nearly isotropic electromagnetic field for the electron. A pearl's circumference is only of length:

$$'O_1 = 2\pi r_1' = \alpha^2 (\pi/2) \lambda_C , \quad (2.2.9)$$

so it follows that the electron characteristic Compton wavelength λ_C must be produced by the core-segments travelling around the spin-loop circumference, which is of length λ_C , thereby modulating the electromagnetic field emitted by the pearls. It might seem that the pearls could be designed as the most basic loop of material, spinning at velocity $(\pi/2)c$ orthogonal to the θ - plane, but they are just one stage in a series of sub-structures.

2.3 Sequential creation of electron spin-loop and core-segments

Given the previous analysis for the core-segment spiralling and acceleration processes, it is an easy matter to scale up the same basic equations for the spin-loop creation. From Eq.(2.1.1) to Eq.(2.1.4) we replace z_{os} by $(z_{es} = z_e/137.036)$, where z_e is the spin-loop final circumference $2\pi r_e$. That is, z_{es} is the original circumference of a spin-loop-seed which contains the 137 original core-segment-seeds z_{os} , see Fig.2.4. So z now represents the instantaneous length of the primeval spin-loop as it spirals open. Replacing r_{os} by r_{es} allows the spiral and velocity equations (2.1.5) to (2.1.8) to represent the spin-loop growth and lead to an action integral analogous to Eq.(2.1.10):

$$\int_{O_{es}}^{O_e} \frac{e^2}{z} \left(1 - \frac{v_z}{c} \right) \left[\frac{v_z}{c} \right] dt \approx \int_0^{2\pi} \frac{m}{2} c r_o d\theta . \quad (2.3.0)$$

Here, each of the 137 core-segment-seeds of charge $(e/137)$ interacts with the whole spin-loop charge e to produce the action of potential energy on the left. This is equal to the total action of kinetic energy for the 137 core-segments shown on the right.

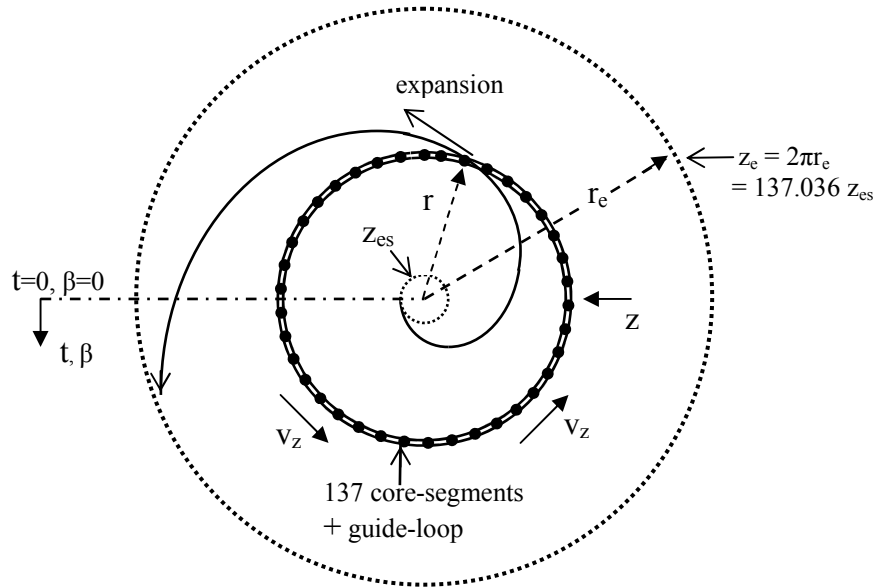


Fig 2.4 Schematic diagram of the spin-loop spiralling process in which the rotating material-loop expands exponentially from a seed radius r_{es} to its final radius r_e .

The spiralling core-segment-seeds are controlled by a circulating electromagnetic field (guide-loop) according to Eq.(2.1.11), wherein h_{os} is replaced by ($h_o = h / 137$). The total spiralling time is $[t_m = t_e \ln(137.036)]$, where ($t_e = 2\pi r_e / c = 137t_o$) is the final equilibrium spin-loop period .

At the end of the spiralling stage, the 137 core-segment-seeds have only velocity $c/(1 + \ln 137.036)$ around the spin-loop circumference and need to be accelerated back to c . This occurs as in Section (2.2), and by analogy with Eq.(2.2.7), the total acceleration time will be set at t_e , see Fig.2.5.

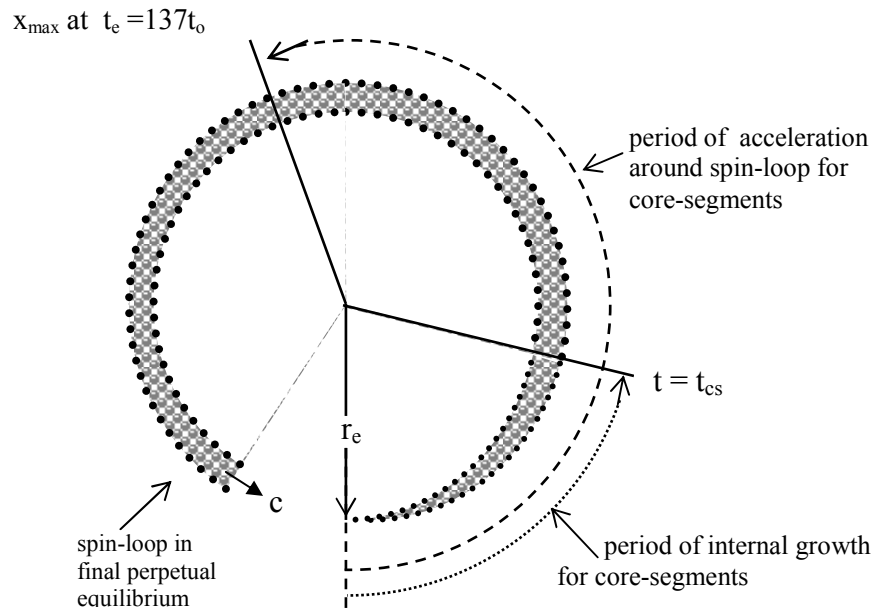


Fig 2.5 Schematic diagram of the spin-loop acceleration process in which the rotating material-loop at radius r_e accelerates from velocity $c/(1+\ln 137)$ to c in time t_e over a distance $2\pi r_e(0.58)$.

It is thought that the core-segment-seeds only start their own *internal* spiralling and acceleration at the beginning of this spin-loop acceleration stage, and complete in total time [$t_{cs} = t_0(1 + \ln 137.036)$] as previously explained.

The original spin-loop-seed may be created from a smaller germ, via Eq.(2.5.15) for example. However, correspondence with a *classical* electron occurs theoretically at the level of a spin-loop-seed. For example, the spin-loop-seed has charge e and radius ($r_{es} = r_e / 137.036 = r_0$), so Eq.(1.5) would apply for the electron field energy. Nevertheless, according to the present model, electron creation does not actually involve compressing charge elements; but theoretical dispersion of the charge to infinity would be permitted energetically.

2.4 Electron spin-loop in equilibrium

After the toroidal spin-loop has been created, the turns/core-segments carry on whirling around the loop in equilibrium ad infinitum, see Fig.2.6. The action over one period of this loop, due to the 137 core-segments, is given by:

$$(m/2)cr_e 2\pi = 137.036(m/2)cr_o 2\pi = h/2 . \quad (2.4.0a)$$

The spin-loop circumference is equal to one Compton wavelength:

$$'O_e = 2\pi r_e = 2\pi r_o (137.036) = h/mc = \lambda_C , \quad (2.4.0b)$$

which implies the continued existence of a material guide-loop to confine the core-segments and ensure the electron's long term stability. The guide-loop's own material energy will be estimated in Section (3) to be around $(\alpha/2\pi)(m/2)c^2$.

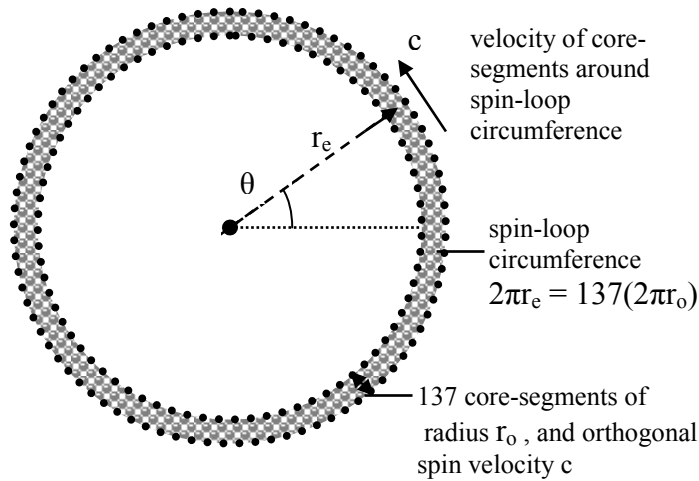


Fig 2.6 Schematic diagram of the spin-loop in final equilibrium at radius r_e , in which the 137 core-segments constitute the helical circumference as they travel along.

A mathematical expression, describing action in the pearls within core-segments during the equilibrium state, may be derived from the following formula:

$$\ln 137^2 \approx \pi^2 . \quad (2.4.1)$$

To develop this, let \tilde{w} be the ratio of two lengths w and w_o with the maximum value ($\tilde{w}_{\max} \approx 137^2$). Then the proposed general form of Eq.(2.4.1) is:

$$(2/\pi)[\ln \tilde{w}]_1^{(137 \times 137)} \approx [\theta]_0^{2\pi} . \quad (2.4.2)$$

Differentiation and multiplication through by $[e^2/c = mcr_0]$ gives:

$$\int_w \frac{e^2}{w} \frac{dw}{c(\pi/2)} \approx 2 \int_0^{2\pi} \left(\frac{m}{2} \right) cr_0 d\theta . \quad (2.4.3)$$

Now, from Section (2.2), the radius of a core pearl is $[r_1' = \alpha r_0 (\pi/2)]$, so let $(w_0 = 2\pi r_1')$ be a pearl circumference. Then $137.036w_0$ is the locus of any given point on a pearl circumference over a core-segment period t_0 , orthogonal to the core-segment plane. Since in the spin-loop there are 137.036 revolutions of each core-segment, the corresponding locus is $(137.036)^2 w_0$ over a complete spin-loop period ($t_e = 137.036t_0$). Given the pearl peripheral velocity $(\pi/2)c$, then $[dw = (\pi/2)c dt]$. And after introducing the core-segment charge $(e/137)$ which interacts with all 137 core-segments in the spin-loop, Eq.(2.4.3) changes to:

$$137 \times \int_{w_0}^{137^2 w_0} \frac{(e^2/137)}{w} dt \approx 137 \times 2 \times \int_0^{2\pi} \left(\frac{m}{2 \times 137} \right) cr_0 d\theta . \quad (2.4.4)$$

The left hand side is an action integral for scalar potential energy of all the pearls in 137 core-segments over their total path around the spin-loop. On the right is the equivalent core kinetic action, which is double the spiralling action during creation, see Eq.(2.3.0).

One interesting feature of the spin-loop is that the helical circumference (of core-segments within the electromagnetic guide-loop) has unitary pitch, since the core-segments spin and travel along at velocity c . The torsion modulus is therefore a maximum (Sokolnikoff and Redheffer, p.315⁸⁾. Briefly, the torsion represents the rate at which a curve twists out of its osculating plane. For a helix, the parametric equations are:

$$x = r_0 \cos \phi, \quad y = r_0 \sin \phi, \quad z = p\phi, \quad (2.4.5)$$

and the torsion is:

$$\tau = \frac{-p}{r_0^2 + p^2} , \quad (2.4.6)$$

which has a maximum modulus $(1/2r_0)$ when $(p = r_0)$. At the same time, the curvature becomes:

$$\chi = \frac{r_o}{r_o^2 + p^2} = \frac{1}{2r_o} . \quad (2.4.7)$$

This condition may signify minimum stress in the guide-loop and spinning pearls constituting the core-segment, and help account for the electron's stability.

2.5 Creation of the pearls

As described in Sections (2.1) and (2.2), an electron core-segment consists of 137 pearls, each of charge $e / 137^2$, radius $[r_1' = \alpha r_o (\pi/2)]$, circumference 'O₁' and period ($t_1 = 'O_1/c'$). This pearl radius can exist only in the finished core-segment since the original core-segment-seed had a radius ($r_{os} = \alpha r_o$) prior to spiralling open, which is too small to accommodate pearls of radius r_1' . The original pearls were therefore small pearl-seeds within the core-segment-seed, which subsequently grew.

The creation spiralling process for each pearl may be derived from the formula:

$$\ln\left(\frac{37.7}{e_n}\right) - \ln\left[1 + \ln\left(\frac{37.7}{e_n}\right)\right] = \left(\frac{\pi}{e_n}\right)^2 . \quad (2.5.0)$$

Here we have introduced factor 37.7 from the electron-pearl structure constant ($\delta = 1/12\pi \approx 1/37.7$) which is not at all arbitrary, but will appear essential in Section 3 for the magnetic moment analysis. To interpret this let $\tilde{\ell}$ be the ratio of two lengths ℓ and ℓ_o with a maximum value (37.7/ e_n) and minimum value unity. The proposed general form of Eq.(2.5.0) is then analogous to Eq.(2.1.2):

$$(2/\pi)\left[\ln \tilde{\ell} - \ln(1 + \ln \tilde{\ell})\right] \frac{(37.7/e_n)}{1} \approx 2\pi/e_n^2 , \quad (2.5.1)$$

which may be differentiated and multiplied through by $[(e/137^2)^2/c = (m/137^4)cr_o]$ to yield:

$$\int_{\ell} \left(\frac{e}{137^2}\right)^2 \left[\frac{1}{\ell} - \frac{1}{\ell(1 + \ln \tilde{\ell})}\right] \frac{d\ell}{c(\pi/2)} \approx 2 \int_0^{2\pi} \frac{mcr_o}{2 \times 137^4} \left(\frac{1}{e_n^2}\right) d\theta . \quad (2.5.2)$$

This is analogous to Eq.(2.1.4) when ℓ is the instantaneous pearl circumference, and $[1/(1 + \ln \tilde{\ell}) = v_{\ell} / c']$ is for the spiralling velocity, as a pearl-seed circumference ($\ell_o = 'O_{1s}'$) expands to a pearl maximum circumference [$'O_1 = 2\pi r_1' = 'O_{1s}(37.7/e_n)$], and $[c' = c(\pi/2)]$. So we have an action integral analogous to Eq.(2.1.10) for a rotating loop of 37 charged material grains, which constitutes the expanding pearl, namely:

$$\int_{'O_{1s}}^{'O_1} \frac{(e/137^2)^2}{\ell} \left\{ 1 - \frac{v_\ell}{c'} \right\} \left[\frac{v_\ell}{c'} \right] dt \approx 2 \int_0^{2\pi} \frac{mcr_o}{2 \times 137^4} \left(\frac{1}{e_n^2} \right) d\theta \quad . \quad (2.5.3)$$

The right hand side of this is referred to the kinetic energy action of a core-segment as standard, but the factor $(1/e_n^2)$ will be linked with quantum wavepackets later.

It is possible to derive a spiral-controlling wave equation similar to Eq.(2.1.11) as follows. Given the spiralling velocity:

$$v_\ell = \frac{d\ell}{dt} = \frac{c'}{[1 + \ln \tilde{\ell}]} \quad , \quad (2.5.4)$$

then upon integration we get:

$$[c't]_0^t = \ell_{ps} \left[\tilde{\ell} \ln \tilde{\ell} \right]_1^{\tilde{\ell}} \quad , \quad (2.5.5)$$

which evaluates to:

$$c't = \ell \ln \tilde{\ell} \quad .$$

This, with Eq.(2.5.4) and $\ell = 2\pi r$, produces:

$$(c't + 2\pi r)v_\ell = 2\pi rc' \quad , \quad (2.5.6)$$

which is analogous to Eq.(2.1.11).

The instantaneous pearl spiral radius is given by:

$$r = r_{1s} \exp(\gamma/2\pi) \quad , \quad (2.5.7)$$

where γ is the spiral angle starting from zero at the seed original radius ($r_{1s} = 'O_{1s}/2\pi$), when $t = 0$ and $v_\ell = c'$. Consequently:

$$\gamma r = c't \quad , \quad (2.5.8)$$

similar to Eq.(2.1.6), implying that the spiralling pearl loop emits a circulating field to guide the expansion process.

Thus, the original pearl-seed has a circumference [$'O_{1s} = 'O_1(e_n/37.7)$], and rotational velocity c' , the same as the final equilibrium pearl's rotation velocity employed in Eq.(2.2.5). But according to Eq.(2.5.4), the pearl material velocity has dropped to $(c'/\ln 37.7)$ by the end of the spiralling period; therefore it is necessary to accelerate the material back to velocity c' around the final pearl circumference. By analogy with Eq.(2.2.6b) then, a given grain(-seed) of the pearl material may have a position x_1 on the pearl circumference such that:

$$x_1 = A_1 t^2 / 2 , \quad (2.5.9)$$

and the instantaneous velocity is ($u_1 = dx_1 / dt$), which increases from [$u_{1o} = c' / (1 + \ln(37.7/e_n))$] to c' in time t_1 say. Then, by analogy with the core-segment acceleration action Eq.(2.2.8a,b), the scalar potential action of the grain(-seeds) during the pearl acceleration stage is independent of time and given by:

$$\int_{x_1} \frac{(e/137^2)^2}{x_1} dt = \frac{(e/137^2)^2}{c} \left(2 \times \ln \frac{37.7}{e_n} \right) = 2 \times \int_{'O_1/(37.7/e_n)}^{'O_1} \frac{(e/137^2)^2}{\chi} \frac{d\chi}{c'} . \quad (2.5.10)$$

The integral on the right is equal to double the scalar potential action of the controlling electro-magnetic field propagating at velocity c' around the spiralling pearl, as implied by Eq.(2.5.8).

Concomitant with Eq.(2.5.0) there is an interesting expression analogous to Eq.(2.2.2) for action of the grainy charge helix around each pearl:

$$\ln 37.7 \approx \pi^2 / e_n , \quad (2.5.11)$$

which develops to:

$$\int_{\xi_0}^{37.7 \times \xi_0} \frac{(e/137^2)^2}{\xi} \frac{d\xi}{c'} \approx 2 \int_0^{2\pi} \frac{mcr_0}{2 \times 137^4} \left(\frac{1}{e_n} \right) d\theta . \quad (2.5.12)$$

Specifically, this expression applies to each pearl in equilibrium following creation, when there are 37 grains of charge (each of radius r_2') travelling around the pearl, describing 37.7 helical turns in the pearl's circumference; ($\xi_0 = 2\pi r_2' = 'O_2$, and $37.7\xi_0 = 'O_1$). The orthogonal velocity around this helix is [$c' = c(\pi/2)$], which is the same as the pearl rotation velocity so the helical locus has unitary pitch and maximum torsion similar to the electron spin-loop Eq.(2.4.6). The factor $(1/e_n)$ is interesting and will be linked with quantum mechanical wavepackets shortly.

Equation (2.5.3) covers the pearl spiralling process very well but there is an alternative wider expression which includes the original pearl-seed action just prior to spiralling:

$$\left\{ \ln \left(\frac{37.7}{e_n} \right) - \ln \left[1 + \ln \left(\frac{37.7}{e_n} \right) \right] \right\} + \ln 37.7 \approx \frac{\pi^2}{2} . \quad (2.5.13)$$

The third term looks like Eq.(2.5.10) but has a different interpretation in this present context. Upon differentiation of this term, then reduction as for Eq.(2.5.3), we get:

$$\int_{'O_{2s}}^{37.7'O_{2s}} \frac{(e/137^2)^2}{\ell} \frac{d\ell}{c'} \quad . \quad (2.5.14)$$

This represents the scalar potential action of the charged circumference $'O_{1s}$ of the original pearl-seed itself (where $d\ell = c'dt$). However, at this stage of development the 37 grains are only grain-seeds of circumference $'O_{2s}$, as explained in the next section. The right hand side of Eq.(2.5.13) reduces to the same as for Eq.(2.5.12), except e_n is replaced by 2. So here, the action of creation spiralling plus the original pearl-seed action is neatly quantised in *total*. Consequently, an interesting interpretation of Eq.(2.5.13) is that pearl-seeds do not exist in any detail until they suddenly take form with their circumferential grain-seeds, then spiral open immediately into pearls just *after* the core-segment has spiralled open

Given that Eq.(2.5.13) has shown how the pearl-seed structure may be created in situ just prior to spiralling open to form a pearl, it is appropriate to question how the *core-segment-seed* of Section (2.1) came into being. An accurate formula applicable to this is:

$$\left\{ \ln\left(\frac{37.7}{e_n}\right) - \ln\left[1 + \ln\left(\frac{37.7}{e_n}\right)\right] \right\} + \ln 137 \approx 2\pi \quad . \quad (2.5.15)$$

The third term may be developed, like Eq.(2.5.14a) but with reference to Eq.(2.2.2), into the scalar potential action of the pearly circumference around the original core-segment-*germ* itself. This germ then spirals outwards by a radial factor $(37.7/e_n)$ to form the core-segment-*seed*. However, one essential feature of Eq.(2.5.15) is that the whole integrated process involves the velocity of light c , rather than $[c' = c(\pi/2)]$ used in the separate processes of Eqs.(2.2.4) and (2.5.2). Therefore after this spiralling, the pearl-seeds must accelerate to spin velocity c' and also accelerate to propagation velocity c around the core-segment-seed.

It is correspondingly possible that the spin-loop-seed of Section (2.3) may be created from a spin-loop-germ in situ, according to Eq.(2.5.15) again. The spin-loop-*germ* would then have a charged circumference of 137 core-segment-*germs* created just prior to spiralling into the spin-loop-*seed* structure. . This could imply by analogy that the original seed-electron has 137 core-segment-seeds around the spin-loop-seed, but no fully-formed

smaller particles. So the series of different particle sizes is originally very short, but increases as space becomes available. This would obviate the problem of "lesser fleas upon little fleas ad infinitum".

The question arises as to how the pearl creation interacts with the core-segment creation. A most appropriate time for the pearl creation would be during the beginning of the core-segment acceleration stage because the core-segment material must change state here to switch from spiralling to acceleration. A link between constants 137.036 and 37.7 may be derived from:

$$137 \approx 37.7[1 + \ln(37.7/e_n)] . \quad (2.5.16)$$

This is unlike any of the previous action expressions, which related potential energy action to kinetic energy action of the core-segment through ($e^2/c = mcr_0$). Upon introducing the grain mass m_2 and the pearl rotation period t_1 plus the velocity of light c , Eq.(2.5.16) becomes:

$$m_2c^2 137t_1 \approx (37.7m_2c^2)[1 + \ln(37.7/e_n)]t_1 . \quad (2.5.17a)$$

The first term on the *right* is the pearl total mass energy m_1c^2 , and the second term is the pearl total creation period τ_1 . Consequently, given that $137t_1$ on the left is the acceleration period t_0 in a core-segment creation process, then:

$$m_2c^2t_0 \approx m_1c^2\tau_1 . \quad (2.5.17b)$$

Thus, the action of a single grain mass m_2 over the core-segment acceleration period t_0 is numerically equal to the action of pearl creation. This is a significant link between 3 electron features showing that adjacent components do actively cooperate via real material processes. There is an analogous expression linking pearl action over the spin-loop creation period with the core-segment action over its creation period:

$$m_1c^2\tau_e \approx m_0c^2\tau_0 . \quad (2.5.18)$$

Finally, a connection with quantum wavepackets is indicated by the presence of amplitude factor e_n in the right hand side of Eqs.(2.5.3) and (2.5.12), as follows. It is believed that the confining guidewaves around the various circumferences may sometimes be harmonics of the fundamental frequency. There are then 2 or 3, etc. wavelengths around the circumference, rather than just one; and this causes the *action* of the material confined by these harmonics to be decreased by e_n , e_n^2 , etc. We are able to calculate the theoretical

spectrum of material quanta and guidewaves which perform this function. For example, consider a spectrum of wavenumbers comprising a theoretical wavepacket of some characteristic wavenumber ($k_a = 2\pi/\lambda_a$), which is given by:

$$g(k) = \left(\frac{e_n}{\pi} \right) \frac{k_a}{(k^2 + k_a^2)} . \quad (2.5.19)$$

Fourier transformation of this spectrum yields the wavepacket amplitude as a function of a position x :

$$\left(\frac{e_n}{\pi} \right) \int_{-\infty}^{\infty} \frac{k_a \cos(kx)}{(k^2 + k_a^2)} dk = e_n \exp(-k_a x) . \quad (2.5.20)$$

For our calculation, the wavepacket should circulate continuously around the reference circumference ($z_0 = 2\pi r_0$) employed in all the action equations, and be at resonance when there are an integral number of wavelengths around this path. So, let x be a characteristic distance $z_0/2\pi$, and we have ($k_a = 2\pi/\lambda_a$) as specified above. Then for ($k_1 x = 1$), wavelength λ_1 occupies one circumference length z_0 and represents a fundamental frequency ($f_1 = c/\lambda_1$). Consequently, the right side of Eq.(2.5.20) has unit value, as required for the weighting of the action on the right of Eq.(2.1.9).

To satisfy amplitude factor (e_n^{-2}) in Eq.(2.5.3), we need to let k_a be k_3 , with ($k_3 x = 3$) in Eq.(2.5.20); then there are three wavelengths λ_3 around z_0 . That is, frequency ($f_3 = c/\lambda_3$) is the third harmonic of f_1 . Similarly, to satisfy amplitude factor (e_n^{-1}) in Eq.(2.5.11), we put ($k_2 x = 2$) in Eq.(2.5.20), then frequency ($f_2 = c/\lambda_2$) is the second harmonic of f_1 , and there are two wavelengths λ_2 around z_0 . In general therefore, there are an integral number of wavelengths around z_0 and the spectrum amplitude or quantum energy decreases with increasing k_a according to Eq.(2.5.19).

An interesting expression for the action of the guidewavepacket around a pearl-seed circumference may be proposed from the formula:

$$\ln 37.7 \approx 2\pi(e_n^{-1} + e_n^{-2} + \dots + e_n^{-\infty}) = 2\pi/(e_n - 1) , \quad (2.5.21)$$

which may be reduced to:

$$\int_{O_{2s}}^{37.7'O_{2s}} \left[\left(\frac{e}{137^2} \right)^2 \left(\frac{1}{2\pi 37.7c} \right) \right] \frac{d\ell}{\ell} \approx 2 \int_0^{2\pi} \frac{mcr_0}{2 \times 137^4 \times 2\pi 37.7} \left(\frac{1}{e_n} + \frac{1}{e_n^2} + \dots + \frac{1}{e_n^\infty} \right) d\theta . \quad (2.5.22)$$

Here, 'O_{2s}' is the grain-seed circumference, and there are 37 of these grain-seeds around the pearl-seed 'O_{1s}'. The square bracket represents the coefficient of *guidewavepacket action* which is (2π37.7)(c/c') times less than the pearl helix *material action* of Eq.(2.5.12). On the right, the geometric series is the sum of all possible harmonic frequency components of the guidewavepacket, from the second harmonic upwards.

There is an analogous expression for the action of the guidewavepacket around a core-segment-*seed* circumference:

$$\ln 137 \approx \pi(1 + e_n^{-1} + e_n^{-2} + \dots + e_n^{-\infty}) = \pi e_n / (e_n - 1) , \quad (2.5.23)$$

which may be reduced to:

$$\int_{O_{1s}}^{137 O_{1s}} \left[\left(\frac{e}{137} \right)^2 \left(\frac{1}{2\pi 137 c} \right) \right] \frac{dz}{z} \approx \int_0^{2\pi} \frac{mcr_o}{2 \times 137^2 \times 2\pi 137} \left(1 + \frac{1}{e_n} + \frac{1}{e_n^2} + \dots \frac{1}{e_n^\infty} \right) d\theta . \quad (2.5.24)$$

Here, 'O_{1s}' is the pearl-seed circumference, and there are 137 pearl-seeds around the core-segment-seed 'O_{0s}'. The square bracket represents the coefficient of guidewavepacket action which is (2π137c/c') times less than the core-segment helix material action of Eq.(2.2.5). On the right, the series covers all harmonic frequency components of the guidewavepacket from the fundamental upwards.

2.6 Creation of grains

Refinements to theory require the existence of structured grain 'particles' around each pearl. These are the individual turns of another smaller helix constituting the pearl periphery, as mentioned previously. The exact theoretical pearl structure constant ($\delta^{-1} = 12\pi \approx 37.7$) is calculable to within 0.11% when using Eqs.(2.5.11), and an exact electron-grain structure constant [$\varepsilon = 1/24 = (\pi/2)\delta$], will now be proposed, as necessary for the magnetic moment analysis.

For example, consider the expression:

$$\ln 24 \approx \pi . \quad (2.6.1)$$

To interpret this, let $\tilde{\rho}$ be the ratio of two lengths ρ and ρ_0 with maximum value ($\tilde{\rho}_{\max} \approx 24$). The proposed general form of Eq.(2.6.1) is then:

$$[\ln \tilde{\rho}]_1^{24} \approx [\theta/2]_0^{2\pi} . \quad (2.6.2)$$

After differentiation and multiplication through by $[(e/137^2 \times 37.7)^2/c = mcr_0 / (137^2 \times 37.7)^2]$ we get:

$$\int_{\rho_0}^{24\rho_0} \frac{(e\alpha^2\delta)^2}{\rho} \frac{d\rho}{c} \approx \int_0^{2\pi} \frac{m\alpha^4\delta^2}{2} cr_0 d\theta \quad (2.6.3)$$

The integral represents action necessary to produce or maintain a charge helix of 24 *mites* around the grain; analogous to the expression for a grainy helix around a pearl in Eq.(2.5.12). Here the mite circumference ($2\pi r_3 = 'O_3 = \rho_0$) is $(24 \times \pi/2)$ times less than the grain circumference ($'O_2 = 2\pi r_1'$) because the term $d\rho/c$ indicates that the mites rotate at velocity c even though they are travelling around the grain circumference at velocity $[c' = c(\pi/2)]$. This may be contrasted with pearls which rotate at velocity c' while travelling around the core-segment at velocity c , see Section (2.2).

There is no obvious expression like Eq.(2.5.0), for the grain creation spiralling process alone, but there is one analogous to Eq.(2.5.13), which includes the original grain-*seed* action just prior to spiralling:

$$[\ln 24 - \ln(1 + \ln 24)] + \ln 24 \approx \pi^2 / 2 \quad , \quad (2.6.4a)$$

or in general:

$$(2/\pi) \left\{ \left[\ln \tilde{\xi} - \ln(1 + \ln \tilde{\xi}) \right]_1^{24} + \left[\ln \tilde{\xi} \right]_1^{24} \right\} \approx \pi \quad . \quad (2.6.4b)$$

Differentiation and introduction of the grain charge give:

$$\int_{'O_{2s}}^{'O_2} \frac{(e\alpha^2\delta)^2}{\xi} \left\{ 1 - \frac{v_\xi}{c'} \right\} \left[\frac{v_\xi}{c'} \right] dt + \int_{'O_{3s}}^{24'O_{3s}} \frac{(e\alpha^2\delta)^2}{\xi_h} dt \approx \int_0^{2\pi} \frac{m\alpha^4\delta^2}{2} cr_0 d\theta \quad . \quad (2.6.5)$$

The first term is an action integral covering the grain spiralling process, similar to expressions for the spin-loop, core-segment and pearl spirals, when the instantaneous grain circumference is ξ which increases from a grain-seed of circumference $'O_{2s}$ to the final grain circumference ($'O_2 = 24 'O_{2s}$), and velocity $[v_\xi \approx c'/(1 + \ln \tilde{\xi})]$. The second term represents scalar potential action of 24 mite-seeds travelling around the grain-seed circumference helix (at velocity $c' = d\xi_h/dt$) just before the grain spiralling process begins. Obviously, these two quantities interact during creation to satisfy the action shown on the right.

Again it is possible to derive a spiral-controlling wave equation similar to Eq.(2.5.6):

$$(c't + 2\pi r)v_{\xi} = 2\pi rc' ; \quad (2.6.6)$$

so there is an energetic circulating field to guide the exponential expansion analogous to Eq.(2.5.8).

At the end of the spiralling process the grain material (24 mite-seeds), has dropped in velocity to $c'/(1 + \ln 24)$, so it has to be accelerated back to velocity c' around the final grain circumference. By analogy with Eq.(2.5.9), a given mite(-seed) may have position x_2 on the grain circumference such that:

$$x_2 = A_2 t^2 / 2 , \quad (2.6.7)$$

and the instantaneous velocity is ($u_2 = dx_2/dt$), increasing from [$u_{20} = c'/(1 + \ln 24)$] to c' in time t_2 say. Then the scalar potential action of the mite(-seeds) during this grain acceleration stage is independent of time, analogous to Eq.(2.5.10) and given by:

$$\int_{x_2} \frac{(e\alpha^2\delta)^2}{x_2} dt = \frac{(e\alpha^2\delta)^2}{c'} (2 \times \ln 24) = 2 \times \int_{O_2/24}^{O_2} \frac{(e\alpha^2\delta)^2}{\eta} \frac{d\eta}{c'} . \quad (2.6.8)$$

On the right is double the action integral for the controlling electromagnetic field propagating at velocity c' around the spiralling grain.

In the last section, it was shown that the pearl creation occurs during the earliest part of the core-segment acceleration stage immediately after the spiralling finished. Consequently it is proposed that the grain creation occurs during the beginning of the pearl acceleration stage.

Just as there is a numerical link between the core-segment constant 137.036 and the pearl constant 37.7 as shown in Eq.(2.5.16), so there is a link between the pearl and grain constants as follows:

$$\ln(37.7/e_n) \times 37.7 \approx 24(1 + \ln 24) . \quad (2.6.11)$$

Upon introducing the mite mass m_3 and the grain rotation period t_2 plus velocity of light c , this becomes:

$$\ln(37.7/e_n) \times (37.7t_2)m_3c^2 \approx (24m_3c^2)(1 + \ln 24)t_2 . \quad (2.6.12)$$

The first bracket on the right is the grain total mass energy, and the second term is the grain total creation period τ_2 . On the left, $(37.7 t_2 = t_1)$ so $[\ln(37.7/e_n)xt_1]$ is equal to the spiralling period of the pearl creation process (τ_{1s}). Thus:

$$m_3 c^2 \tau_{1s} \approx m_2 c^2 \tau_2 , \quad (2.6.13)$$

and the action of a single mite mass m_3 during the pearl spiralling period is numerically equal to the action of grain creation. This important result links pearl, grain, and mite processes during electron creation.

2.7 Creation of mites

It is thought that mites contain the ultimate charged particles which emit the electron's electric field quanta whereas grains, pearls, core-segments and the spin-loop are hierarchical structures. Each species constitutes the circumferential orbit of the next higher species and is held in place by an electromagnetic guide-loop. Thus an electron consists of $(137^2 \times 37 \times 24)$ mites in four types of orbit, emitting field quanta in all directions on average, although the mass flow around the spin-loop remains orientated, defining the electron spin axis. A mite 'particle' is one of 24 loops of material (radius r_3) around a grain and it consists of 50 elemental 'particle' sources. The electron-mite structure constant is defined as $[\mu = (1/16\pi) \approx 1/50]$ according to the magnetic moment analysis in Section 3.

The mites may evolve by spiralling from their embryo state according to a formula like Eq.(2.6.4), namely:

$$\{\ln 50 - \ln[1 + \ln 50]\} + \ln 50 \approx 2\pi , \quad (2.7.1)$$

or in general:

$$[\ln \tilde{\rho} - \ln(1 + \ln \tilde{\rho})]_1^{50} + [\ln \tilde{\rho}]_1^{50} \approx 2\pi . \quad (2.7.2)$$

After differentiation and introduction of the mite charge we obtain by analogy with Eq.(2.6.5):

$$\int_{O_{3s}}^{O_3} \frac{(e\alpha^2 \delta \varepsilon)^2}{\rho} \left\{ 1 - \frac{v_p}{c} \right\} \left[\frac{v_p}{c} \right] dt + \int_{O_{3s}/50}^{O_{3s}} \frac{(e\alpha^2 \delta \varepsilon)^2}{\rho_h} dt \approx 2 \int_0^{2\pi} \frac{m\alpha^4 \delta^2 \varepsilon^2}{2} c r_0 d\theta . \quad (2.7.3)$$

Here, the first term covers spiralling action for the mite increasing from a seed circumference O_{3s} to its final circumference $[O_3 = 50O_{3s}]$. The second term represents

scalar potential action of 50 element-seeds travelling around the mite-seed circumference helix at velocity c , prior to the spiralling process.

At the end of the spiralling stage the material velocity has dropped to $c/(1 + \ln 50)$ and needs to be accelerated back to c around the final mite circumference. For an acceleration period ($t_3 = 2\pi r_3/c$) say, the instantaneous position of any element(-seed) on the circumference is:

$$x_3 = A_3 t^2 / 2 . \quad (2.7.4)$$

The instantaneous velocity is ($u_3 = dx_3/dt$), increasing from [$u_{30} = c/(1 + \ln 50)$] to c , in time t_3 say. The scalar potential action of the mite material during this acceleration stage is independent of time and is given by:

$$\int_{x_3} \frac{(e\alpha^2 \delta \epsilon)^2}{x_3} dt = \frac{(e\alpha^2 \delta \epsilon)^2}{c} (2 \times \ln 50) = 2 \times \int_{O_3/50}^{O_3} \frac{(e\alpha^2 \delta \epsilon)^2}{\rho} dt , \quad (2.7.5)$$

where the right hand side is double the scalar potential action for the controlling electromagnetic field propagating at velocity c around the spiralling mite.

The helix of 50 elements, spinning at velocity c while propagating at velocity c around a mite circumference, may be described by developing the formula:

$$\ln 50 \approx \pi(\pi/e_n) . \quad (2.7.6)$$

Factor (π/e_n) has been employed elsewhere to account for the confining guidewave energy which is associated with the material energy. Thus, the scalar potential action of the 50 elements is approximately:

$$\int_{\sigma_0}^{50\sigma_0} \frac{(e\alpha^2 \delta \epsilon)^2}{\sigma} dt \approx \left(\frac{\pi}{e_n} \right) \times \int_0^{2\pi} \frac{m\alpha^4 \delta^2 \epsilon^2}{2} c r_0 d\theta . \quad (2.7.7)$$

Analogous to Eq.(2.5.16), there is a numerical link between the grain and mite constants as follows:

$$(\pi/e_n)(1 + \ln 24) \approx (1 + \ln 50) . \quad (2.7.8)$$

By introducing the element mass m_4 and the mite rotation period t_3 plus velocity of light c , then rearranging, this becomes physically meaningful:

$$50(\pi/e_n)m_4 c^2 [(1 + \ln 24)(24t_3)] \approx (24m_3 c^2)[(1 + \ln 50)t_3] . \quad (2.7.9)$$

The first bracket on the right is the mass energy of 24 mites in a grain, and the second term is the mite total creation period τ_3 . On the left, $(24t_3 = t_2)$, so $(1+\ln 24)t_2$ is the total grain creation time τ_2 . Then:

$$50(\pi/e_n)m_4c^2\tau_2 \approx 24m_3c^2\tau_3, \quad (2.7.10)$$

where the action of 50 elements (including the guidewave energy term (π/e_n)) over one grain creation period is equivalent to the creation action of 24 mites. Clearly, every part of the electron is actively connected with adjacent parts during the creation processes.

The final elements themselves may evolve by spiralling from their own embryo state according to a formula like Eq.(2.5.0), namely:

$$\left\{ \ln\left(\frac{50}{e_n}\right) - \ln\left[1 + \ln\left(\frac{50}{e_n}\right)\right] \right\} \approx \frac{\pi}{2}, \quad (2.7.11)$$

or in general:

$$[\ln \tilde{\omega} - \ln(1 + \ln \tilde{\omega})]_1^{50/e_n} \approx \frac{\pi}{2}. \quad (2.7.12)$$

After differentiation and introduction of the element charge we obtain by analogy with Eq.(2.5.3):

$$\int_{O_{4s}}^{O_4} \frac{(e\alpha^2\delta\epsilon\mu)^2}{\omega} \left\{ 1 - \frac{v_\omega}{c} \right\} \left[\frac{v_\omega}{c} \right] dt \approx \frac{1}{2} \int_0^{2\pi} \frac{m\alpha^4\delta^2\epsilon^2\mu^2}{2} c r_o d\theta. \quad (2.7.13)$$

Here, the term on the left covers spiralling action for the element increasing from a seed circumference O_{4s} to its final circumference $[O_4 = O_{4s}(50/e_n)]$. This spiralling growth begins as soon as the mite has finished its spiralling. Like the other species, these elements are simply the turns of material which constitute a continuous helix.

Our electron model with five different species of helically-wound 'particles' is certainly complex, but satisfies the accurate empirical values of α and anomalous magnetic moment. The smaller species are of interest because of the link with quantum wavepackets. One consequence of the reduction in particle number per orbit from 137 through 37 to 24 is reduced energy density within the particle seeds prior to spiralling.

A noticeable feature of the analyses for the 5 systems is their near independence of one another. Each species rotates orthogonally to, but around the next larger species' circumference. It must be fundamental that the structure constants are 12π , 24 , and 16π ,

with links like Eqs.(2.5.16), (2.6.11), (2.7.8), and (2.4.4). And, it is remarkable that the numerous processes should all be so individually quantised in their actions, although the continuity details remain unknown because the equations only involve finite integrals.

2.8 Electron charge uniqueness

Previous calculations of creation action depended upon the charge being divisible among the various sub-structures; so we need a formula to describe the fundamental charge of the elements in an electron. One has been found which is based upon allocating 3 fragments of charge Δq to each element. These may be visualised as 3 localised material curls constituting the element circumference. In addition, there needs to be some field material holding the 3 charge-curls in place, effectively increasing their weight to $3(\pi/e_n)$. Now the total number of elements per electron is:

$$n_e = 137 \times 137 \times 37.7 \times 24 \times 50 = 8.540466 \times 10^8 \quad . \quad (2.8.1)$$

The electron total charge is therefore:

$$e = n_e \times 3(\pi/e_n) \times \Delta q = 2.961135 \times 10^9 \Delta q \quad . \quad (2.8.2)$$

Prior to confining them in the electron, let all the charge-curls be situated in a helix constituting a single circumferential loop. Then, electromagnetic action over all these will be based upon the formula:

$$\ln\{n_e \times 3(\pi/e_n)\} \approx 3(\pi/e_n)2\pi \quad . \quad (2.8.3)$$

Upon introducing ($e^2/c = m_e c r_{oe}$) as previously, the action around this loop material, which has the form of a circumferential helix of cross-sectional radius r_q and unitary pitch, may be expressed:

$$\int_x \frac{e^2}{x} dt \approx 3 \left(\frac{\pi}{e_n} \right) \times \int_0^{2\pi} m_e c r_{oe} \quad , \quad (2.8.4)$$

where x varies from $2\pi r_q$ to $2\pi r_q [n_e \times 3(\pi/e_n)]$, and ($dt = dx/c$). This primeval loop of around 3×10^9 charge-curls is a most basic definition of *charge e*. Factor 3 on the right may indicate that electronic charge e could agglomerate into three linked pieces, but empirical evidence for ($e/3$) is unconfirmed.

3 Electron anomalous magnetic moment

For the basic electron model of Eq.(1.7), the spin-loop would be expected to produce a magnetic moment of 1 Bohr Magneton,

$$\mu_B = \text{current} \times \text{area} = \left(\frac{ec}{2\pi r_e} \right) \left(\pi r_e^2 \right) = \frac{e\hbar}{2m} . \quad (3.1)$$

However, the measured magnetic moment μ_e is found to be greater than μ_B , the latest result being:

$$\mu_e / \mu_B = 1.00115965218111(74). \quad (3.2)$$

Our electron model produces an expression which is relatively concise and easy to comprehend:

$$\begin{aligned} \mu_e / \mu_B &= \{1 + [2\pi\alpha^{-1} + 1]^{-1}\} \{1 - \alpha^3 [1 + 2\delta(1 + (2/\pi)\varepsilon[1 + \mu(2/\pi)])]\} \\ &= 1.00115965218149(80) . \end{aligned} \quad (3.3)$$

Here the fine structure constant has been taken as the current measured value:

$$\alpha^{-1} = 137.035999679(94) , \quad (3.4)$$

and the theoretical pearl structure constant from Section (2.5) is ($\delta = 1/12\pi \sim 1/37.7$), and the grain structure constant from Section (2.6) is ($\varepsilon = 1/24$) exactly, and the mite structure constant from Section (2.7) is ($\mu = 1/16\pi \sim 1/50$). In Eq.(3.3) the error term is determined by α and demonstrates the paramount importance of its experimental determination.

Each part of Eq.(3.3) has a particular function, explicable in terms of the previous detailed electron model.

(a) The most significant term is the first curly bracket on the right which represents total electric field energy, including that in the spin-loop guidewave. It was shown in Eq.(1.5) that the total energy of the electron's external electric field is $(1/2)mc^2$, so that the remaining half of the electron's energy must reside in the core-segments and spin-loop guidewave. Now the electric self-interaction energy of the electron due to the spin-loop is around $e^2/(2\pi r_e)$, as calculated by using the method of Eq.(1.6). But this energy has to be supplied by the electron itself, so the self-interaction energy is actually reduced slightly to:

$$\Delta E = (e^2 / 2\pi r_e)(1 - \Delta E / mc^2) , \quad (3.5)$$

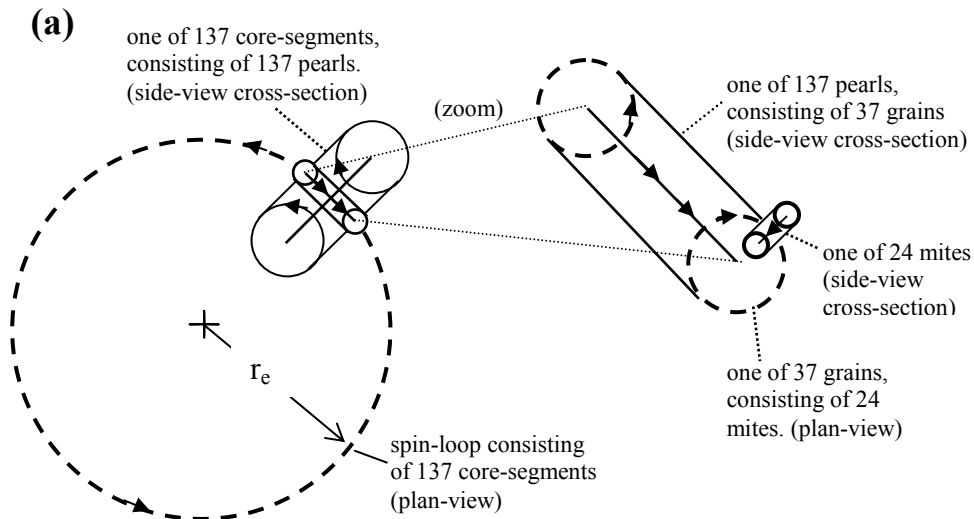
therefore:

$$\Delta E / mc^2 = (2\pi\alpha^{-1} + 1)^{-1}, \quad (3.6)$$

Half this energy returns to the external electric field but the other half constitutes the guidewave energy within the spin-loop, which has the same nature as the electric field.

Consequently, the electron magnetic moment should approach: $e(1 + \Delta E / mc^2)(\hbar / 2m)$.

(b) The second curly bracket contains correction terms due to the finite areas of pearls, grains, mites, and elements, which produce their own magnetic moments. These are all effectively antiparallel to the spin-loop, according to the minus sign. Core-segments travel around the spin-loop circumference at velocity c but are oriented orthogonally to the circumference, so contribute zero magnetic moment to the electron, see Figs.3.1a,b.



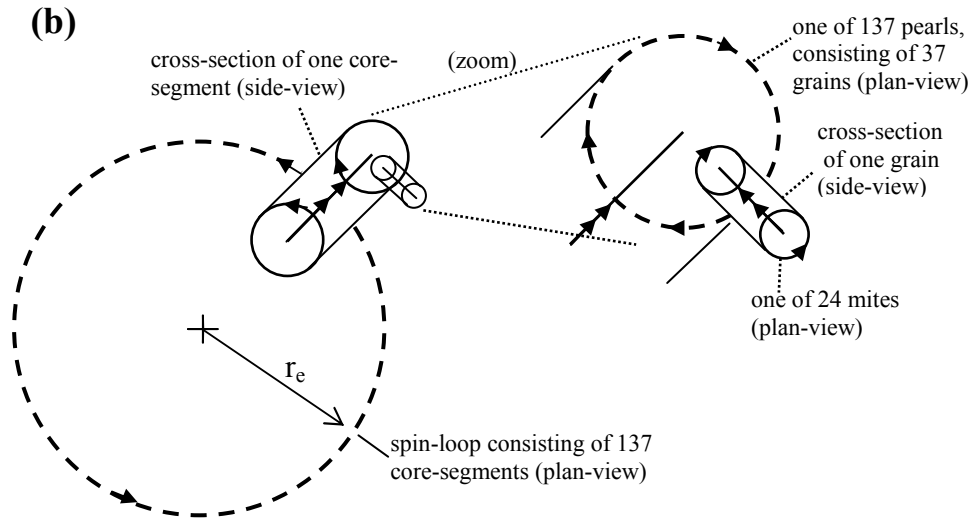


Fig.3.1a,b Schematic diagrams of a cross-sectional plan-view of the electron spin-loop, showing only one of the core-segments, with one pearl containing one grain and one mite. Drawn not-to-scale, in order to illustrate the orthogonal structure of the assembly and directions of travel for all particles.

The anti-parallel nature of the pearls, grains, mites and elements relative to the spin-loop magnetic moment has to be attributed to helicity rather than orientation, since these particles continually change direction in 3 dimensions during their travels. As illustrated, given left-handed helicity for all the electron particles, the pearls rotate through the centre of a core-segment in the same direction as core-segment propagation. Similarly, the grains rotate through a pearl centre in the direction of pearl propagation: likewise for mites rotating through a grain centre. This kind of co-rotation relative to propagation will be taken to represent a minimum energy condition. A positron has right-handed helicity throughout, and its component particles exhibit the same *relative* alignments as for an electron. Consequently, Eq.(3.3) covers positrons and electrons equally. Physical meaning may be attributed to each part of the second curly bracket, by reduction to its proposed original form, as follows:

$$\left\{ 1 - \left(\frac{1}{137} \right) \left(\frac{2}{\pi} \right)^2 \left[\frac{137^2}{137^4 (2/\pi)^2} \right] \left[1 + 2 \left(\frac{37.7}{37.7^2} \right) \left(1 + \left(\frac{\pi}{2} \right) \frac{24}{(24\pi/2)^2} \left[1 + \left(\frac{2}{\pi} \right) \frac{50}{50^2} \right] \right] \right] \right\}. \quad (3.7)$$

137x137 pearls 37 grains 24 mites 50 elements

For clarity, approximate forms of α , δ , ϵ , μ have been shown here.

Primary factor (1/137) is believed to represent the interaction coefficient between the helical particle orbits and an external magnetic field: that is, 137 times weaker than for the standard loop magnetic moment of (current x area). Coupling factor $(2/\pi)^2$ is to do with helicity/perspective, and will be explained more effectively later.

The first square bracket describes the total magnetic moment of 137^2 pearls in 137 core-segments around a spin-loop. Each pearl has area $[137^2(2/\pi)]^2$ times less than the spin-loop area. Current around a pearl is determined to be the same as around the spin-loop:

$$i_1 = q_1 c' / 2\pi r_1' = ec / 2\pi r_e, \quad (3.8)$$

where $(q_1 = e/137^2)$, $[c' = c(\pi/2)]$ and $[r_1' = r_e (\pi/2)/137^2]$.

The second square bracket contains analogous terms for grains and mites. Factor $(37.7/37.7^2)$ covers 37.7 effective number of grains per pearl, each of area $(37.7)^2$ times less than a pearl area. Current around a grain is the same as around a pearl:

$$i_2 = q_2 c' / 2\pi r_2' = ec / 2\pi r_e, \quad (3.9)$$

since $(q_2 = q_1 / 37.7)$ and $(r_2' = r_1' / 37.7)$. Coefficient 2 implies that the grain magnetic moment is twice the expected value, compared with the pearl magnetic moment. This interpretation is supported by Eq.(2.5.11) which describes action of the grainy charge helix around a pearl. Double energy is denoted on the right there, relating to a second harmonic guidewave.

Factor $24/(24\pi/2)^2$ covers 24 mites per grain, each of area $(24\pi/2)^2$ times less than a grain area. Current around a mite is also the same as around a pearl:

$$i_3 = q_3 c / 2\pi r_3 = ec / 2\pi r_e, \quad (3.10)$$

since $(q_3 = q_2 / 24)$, and $[r_3 = r_2' / (24\pi/2)]$. A possible explanation for the weighting factor $(\pi/2)$, could be connected with the mite helicity since its spin velocity is c while it propagates at velocity c' around its grain circumference.

In the third square bracket, factor $50/50^2$ covers the 50 effective-number of elements per mite, each of area 50^2 times less than a mite area. Prefix $(2/\pi)$ is to cancel the previous $(\pi/2)$ weighting factor, since the element rotation velocity c is the same as its propagation velocity around the mite. Current around an element is the same as around a pearl:

$$i_4 = q_4 c / 2\pi r_4 = ec / 2\pi r_e \quad , \quad (3.11)$$

since $(q_4 = q_3 / 50)$, and $(r_4 = r_3 / 50)$. This means that the current flows in series through every element, mite, grain, pearl and core-segment: analogous to a light bulb with a quintuply-coiled filament.

Finally, the attenuation coefficient $(2/\pi)^2$ at the beginning applies directly to grains, mites and elements because of their changes in orientation as they move. Their areas, projected parallel to the spin-loop, are reduced to $(2/\pi)$ on average in *two* axes. Pearls however, in their motion around a core-segment, only suffer reduction in projected area by $(2/\pi)$ on average. Consequently, the additional factor $(2/\pi)$ could be due to helicity in that the pearl spin velocity is c' while its propagation velocity is only c around a core-segment; logically similar to the mite multiplier $(\pi/2)$ just mentioned.

Before leaving this subject, it is interesting to compare Eq.(3.3) with the equivalent QED anomaly expression (Gabrielse et al, ⁹⁾:

$$a(\text{QED}) = 0.5 \left(\frac{\alpha}{\pi} \right) - 0.328478965579 \left(\frac{\alpha}{\pi} \right)^2 + 1.181241456587 \left(\frac{\alpha}{\pi} \right)^3 + \dots \quad (3.12)$$

If Eq.(3.3) is expanded as a series in (α/π) , without including δ , ε , μ , terms, we get:

$$a(\text{Eq.(3.3)}) = \frac{1}{2} \left(\frac{\alpha}{\pi} \right) - \frac{1}{4} \left(\frac{\alpha}{\pi} \right)^2 + \left(\frac{1}{8} - \pi^3 \right) \left(\frac{\alpha}{\pi} \right)^3 + \dots \quad (3.13)$$

Clearly, these square and cubic terms differ from Eq.(3.12), which implies that the QED method is not compatible with this real model. Our square term comes only from the first curly bracket of Eq.(3.3) and is independent of the cubic term.

4 Refinements to creation formulae and fine structure constant

4.1 Creation formulae

For simplicity, all electron structure equations (2.1.1), (2.2.1) and (2.5.0) etc. were used in their approximate forms throughout the analyses of previous sections. However,

some small extra terms were neglected, which are thought to represent the interaction of different systems during the spiralling and equilibrium states, in addition to any guidewave energy corrections. In Section (3) it was shown that the electron anomalous magnetic moment may be partly attributed to the effect of spin-loop guidewave energy, approximately $\Delta E = mc^2/(2\pi 137)$. So terms of this order are expected to involve α , δ , ε , μ , depending on the system described. Work remains to be done on interpreting these correction terms, but in each case a single correction term has been sought, which looks familiar and increases the overall accuracy greatly.

Accuracy of the electron model is governed by the fine structure constant, and this is now very precise:

$$\alpha^{-1} = 137.035999679(94) \quad . \quad (4.1.1)$$

Then the electron core-segment creation spiral equation (2.1.1) may be much more accurately written so as to include a term to increase the action of a core kinetic energy:

$$\ln \alpha^{-1} - \ln(1 + \ln \alpha^{-1}) \approx \pi(1 + \alpha^2 \pi / 2) \quad , \quad (4.1.2)$$

Similarly, the expression for action of the pearly helix, derived from Eq.(2.2.2) may be greatly improved in accuracy by subtracting a small term:

$$\ln \alpha^{-1} \approx \pi^2 / 2 - 2\alpha \quad . \quad (4.1.3)$$

Pearl creation equations (2.5.0) and (2.5.13) may be more accurately written:

$$\left\{ \ln \frac{37.7}{e_n} - \ln \left[1 + \ln \frac{37.7}{e_n} \right] \right\} \approx \left(\frac{\pi}{e_n} \right)^2 \left(1 + \frac{\alpha}{2} \right) \quad , \quad (4.1.4)$$

$$\left\{ \ln \frac{37.7}{e_n} - \ln \left[1 + \ln \frac{37.7}{e_n} \right] \right\} + \ln 37.7 \approx \left(\frac{\pi^2}{2} \right) (1 + \alpha) \quad . \quad (4.1.5)$$

These small additions could represent interactions between species. Equation (2.5.11) has a small correction term, which could be related to guidewave action keeping the grains in orbit around a *final* pearl:

$$\ln 37.7 \approx \pi^2 / e_n - (\alpha / 2\pi) \quad . \quad (4.1.6)$$

Grain creation equations (2.6.1) and (2.6.4a) are more accurately expressed:

$$\ln 24 \approx \pi + \alpha(\pi^2 / 2) \quad . \quad (4.1.7)$$

$$[\ln 24 - \ln(1 + \ln 24)] + \ln 24 \approx (\pi^2 / 2) - \alpha(\pi / e_n) \quad , \quad (4.1.8)$$

Mite creation equations (2.7.1) and (2.7.6) are greatly improved as:

$$\left[\ln 50 - \ln(1 + \ln 50) \right] + \ln 50 \approx 2\pi - \alpha(\pi^2 / 2) , \quad (4.1.9)$$

$$\ln 50 = \pi(\pi / e_n)(1 + 1/4\pi) . \quad (4.1.10)$$

Element evolution equation (2.7.11) is accurately:

$$\left\{ \ln\left(\frac{50}{e_n}\right) - \ln\left[1 + \ln\left(\frac{50}{e_n}\right)\right] \right\} \approx \frac{\pi}{2} \left(1 - \frac{1}{2\pi}\right) , \quad (4.1.11)$$

Finally, charge uniqueness equation (2.8.3) includes a term like the anomalous magnetic moment expression Eq.(1.10):

$$\ln\{n_e \times 3(\pi / e_n)\} \approx 3(\pi / e_n)2\pi[1 + \alpha / 2\pi] . \quad (4.1.12)$$

4.2 Detailed expression for the fine structure constant

Electrons are identical, stable and of complex structure, which means that their inherent substance is vigorous during expansion from a simpler seed state but this is limited to a very precise size and shape. The fine structure constant has been applied to the electron creation phenomenon via two theoretical conditions, Eqs.(2.1.1) and (2.2.1). A physical relationship which also looks fundamental is that half the electron's energy ($E/2$) resides in its external field, so nominally ($E/2 = mc^2/2 = e^2/2r_0$). This had to be introduced arbitrarily into Eq.(2.1.4) to make it physically meaningful. Hence 137.036 is certainly a growth factor, which may be controlled by fitting one Compton guidewavelength around the spin-loop, ($2\pi r_e = h/mc = hc/E$). This would establish a subjective link [$(r_e / r_{es}) = 137.036 = (hc/e^2)$]. However, a free choice for Planck's constant alone, or of charge, or velocity of light, would not guarantee satisfying this link via Eq.(2.1.1). So for electrons to exist, their design must satisfy Eq.(2.1.1) primarily as applied to spin-loop *creation* action, but with minor contributions from other species because of their finite sizes. For empirically determined α in Eq.(4.1.1), we may derive a more accurate interpretation of Eq.(2.1.1) in its logarithmic or 'action' form:

$$\left\{ \ln \alpha^{-1} - \ln\left(1 + \ln \alpha^{-1}\right) \right\} = \pi \left\{ 1 + \frac{\pi \alpha^2}{2} \left[1 + \frac{\pi \delta}{2} \left(1 - \frac{2\varepsilon}{\pi} \left\{ \frac{\pi}{e_n} \right\} \right) \right] \right\} . \quad (4.2.1)$$

Expansion of the right side and introduction of (mcr_0) produces familiar terms for the different species:

$$\frac{m}{2} c_{r_0} 2\pi \left\{ 1 + \frac{137^2}{137^4} \left(\frac{\pi}{2} \right)_{c'r'}^2 \left[\left(\frac{2}{\pi} \right)_h + \frac{37.7}{37.7^2} \left(1 - \left(\frac{\pi}{2} \right)_h \frac{24}{24^2} \left(\frac{2}{\pi} \right)_{cr}^2 \left\{ \frac{\pi}{e_n} \right\} \right] \right\}. \quad (4.2.2)$$

Approximate forms for α , δ , and ε have been shown for clarity, only.

Since all the creation expressions in previous sections are written as functions of $[(m/2)c_{r_0}2\pi]$, we will assume that angular momentum is especially involved in the correction terms. The principle term (factor 1) then covers the spin-loop spiralling, and could mean that corrections are to be referred to the spin-loop. If so, the core-segments, which travel around the spin-loop orthogonally to it, do not appear to contribute any correction term. In contrast, the pearls are parallel to the spin-loop some of the time and could account for the first correction factor, as follows. There are 137^2 pearls per spin-loop and their creation action is always reduced by 137^4 in Section (2.5). Factor $(\pi/2)_{c'r'}^2$ is taken to cover the pearl's superluminal spin velocity [$c' = c(\pi/2)$], plus its concomitant increase in radius [$r_1' = r_1(\pi/2)$]. In the square bracket, $(2/\pi)_h$ is believed to represent the helicity coupling coefficient due to the pearl propagation velocity being c while it spins at c' , (compare with Eq. (3.7)).

The next correction term is due to 37.7 grains per pearl, weighted by $(\alpha^4 \delta^2)$ as in all creation action expressions in Section (2.6). Previous factor $(\pi/2)^2$ applies as for the pearls, but the helicity coupling coefficient is unity for grains which spin and also propagate at velocity c' .

The next correction term is due to 24 mites per grain, weighted by $(\alpha^4 \delta^2 \varepsilon^2)$ as in all creation action expressions of Section (2.7). Factor $(2/\pi)_{cr}^2$ is to nullify the earlier $(\pi/2)^2$ because mites spin at velocity c and have concomitant reduced radius r_3 . Coefficient $(-\pi/2)_h$ is interpreted again as being due to helicity, but in this case the mites propagate at velocity c' while spinning at c . Factor (π/e_n) is attributed to the 50 elements in each mite, with their confining guidewave energy included.

The spin-loop equilibrium expression Eq.(2.4.1) defines α perpetually. Obviously, this is the fine structure constant we must encounter in physics, when the electron has settled into its final state. An accurate definition, again including minor contributions from other species, is:

$$\left(\frac{2}{\pi}\right) \ln 137^2 = 2\pi \left\{ 1 - \alpha \left(\frac{2}{\pi}\right)^2 \left[1 - \alpha \left(\frac{1}{\pi}\right) \left(1 + \delta \left(\frac{\pi}{2}\right)^2 \left\{ 1 + \varepsilon \left(\frac{2}{\pi}\right)^2 \left(\frac{\pi}{e_n}\right) \right\} \right) \right] \right\}. \quad (4.2.3)$$

Obviously this is more involved than Eq.(4.2.1), but we can roughly interpret what is being described. Expansion of the right side and introduction of (mcr_o) produces familiar terms for the different species:

$$2\frac{m}{2} cr_o 2\pi \left\{ \left[1 + \frac{137}{137^2} \left(\frac{2}{\pi}\right)_{cr}^2 \left(\frac{2}{\pi}\right)_a \times \left[\left(-\frac{\pi}{2}\right)_h + \frac{137}{137^2} \left(\frac{\pi}{2}\right)_{c'r'}^2 \left(\frac{2}{\pi}\right)_h \left(\frac{1}{2}\right) \left(\frac{2}{\pi}\right)_a + \frac{37.7}{37.7^2} \left\{ \left(\frac{\pi}{2}\right)_{h'} + \frac{24}{24^2} \left(\frac{2}{\pi}\right)_{cr}^2 \left(\frac{\pi}{2}\right)_h \left(\frac{\pi}{e_n}\right) \right\} \right] \right] \right\}. \quad (4.2.4)$$

The principle term (factor 1) covers spin-loop action, expressed in terms of its 137^2 constituent pearls, as in Eq.(2.4.1). Following this, most correction occurs in the spin-loop where there are 137 core-segments, with action reduced by 137^2 , as in Eq.(2.1.10). Factor $(2/\pi)_{cr}^2$ recovers the core-segment normal radius and velocity of light, from the previous latent pearl values $c'r_1'$. Factor $(2/\pi)_a$ did not appear in Eq.(4.2.2) and is thought to represent an average or perspective view of circular motion as in Eq.(3.7). In the following square bracket, $(-\pi/2)_h$ is the helicity coupling coefficient, due to the core-segment spinning and propagation velocities both being c , contrary to the previous pearl.

The next correction term is due to 137 pearls per core-segment, with $c'r_1'$ reinstated by the factor $(\pi/2)_{c'r'}^2$, plus a corresponding helicity coefficient $(2/\pi)_h$. An extra weighting factor $(1/2)$ is also necessary, in addition to a further average/perspective factor $(2/\pi)_a$, in the following round bracket.

The next correction term is due to 37.7 grains per pearl, weighted by $(\pi/2)_{h'}$ in the following curly bracket to nullify the previous helicity coefficient because grains spin and propagate at velocity c' . No change in $c'r'$ is therefore necessary here.

The final correction term is due to 24 mites per grain, with $(2/\pi)_{cr}^2$ for decrease in spin velocity and radius, plus corresponding $(\pi/2)_h$ helicity coefficient. As in Eq.(4.2), factor (π/e_n) is attributed to the 50 elements in each mite, with their confining guidewave energy included.

In conclusion, the experimental fine structure constant is governed primarily by the electron equilibrium spin-loop equation, but this depends on the creation spiral in addition to other species contributing to its exact value. The action of spiralling by itself does not define α because it is the electromagnetic guidewave which locks-in to *prevent* further expansion when $(2\pi r_e = \lambda_c)$ is reached.

5 Conclusion

A detailed model of electron structure in 5 levels has been developed, based on the empirical fine structure constant and anomalous magnetic moment. Properties such as charge, mass and spin can now be understood classically in 4-dimensional space-time as real physical features. Calculation of the experimental value of anomalous magnetic moment is relatively straightforward in geometrical terms. Un-natural concepts like negative energy, renormalisation, compactification, and Higgs bosons have not been necessary in this physical model.

Further work on muon, proton and neutron structure, using methods developed here, is in progress and appears very encouraging. These particles also consist of localised energy/material travelling in helixes at the velocity of light, thereby excluding Higgs bosons.

Acknowledgements

I would like to thank Imperial College Libraries, A.Rutledge for typing and R. Glovnea for computing assistance.

References

- 1) Wiki , "http://en.wikipedia.org/wiki/Toroidal_ring_model", (2010).
- 2) D. L. Bergman and J. P. Wesley, Galilean Electrodynamics, **1**, (1990), 63.
- 3) W. H. Bostick , Physics Essays, **4**, (1991), 45.
- 4) R. Wayte, Astrophys. Space Science, **91**, (1983), 345.
- 5) L. D. Landau and E. M. Lifshitz, The Classical Theory of Fields, Pergamon, Oxford, (1975).

- 6) P. A. M. Dirac, *The Principles of Quantum Mechanics*, Oxford Clarendon Press, (1962).
- 7) L. I. Schiff, *Quantum Mechanics*, McGraw-Hill, N York, (1968).
- 8) I. S. Sokolnikoff and R. M. Redheffer, *Mathematics of Physics and Modern Engineering*, McGraw-Hill, N York, (1958).
- 9) G. Gabrielse, et al, *Phys. Rev. Lett.*, (2006), **030802**.